UNCLASSIFIED

AD NUMBER
AD524398
CLASSIFICATION CHANGES
TO: **UNCLASSIFIED**
FROM: **SECRET**
LIMITATION CHANGES
TO: **Approved for public release; distribution is unlimited.**
FROM: **Distribution authorized to U.S. Gov't. agencies and their contractors; Administrative/Operational Use; DEC 1972. Other requests shall be referred to Defense Advanced Research Projects Agency, 675 North Randolph Street, Arlington, VA 22203-2114.**
AUTHORITY
RADC ltr dtd 16 Jul 1974; RADC ltr dtd 16 Jul 1974

THIS PAGE IS UNCLASSIFIED

SECURITY
MARKING

The classified or limited status of this report applies to each page, unless otherwise marked.
Separate page printouts MUST be marked accordingly.

THIS DOCUMENT CONTAINS INFORMATION AFFECTING THE NATIONAL DEFENSE OF THE UNITED STATES WITHIN THE MEANING OF THE ESPIONAGE LAWS, TITLE 18, U.S.C., SECTIONS 793 AND 794. THE TRANSMISSION OR THE REVELATION OF ITS CONTENTS IN ANY MANNER TO AN UNAUTHORIZED PERSON IS PROHIBITED BY LAW.

SECRET

AD524398

RADC-TR-73-15
Final Technical Report
December 1972

SCATTERING MODEL DEVELOPMENT (U)

Raytheon Company

"NATIONAL SECURITY INFORMATION"

"Unauthorized Disclosure Subject to Criminal Sanctions"

Sponsored by
Defense Advanced Research Projects Agency
ARPA Order No.1423

[redacted]

The views and conslusions contained in this document are those of the authors and should not be interpreted as necessarily representing the official policies, either expressed or implied, of the Defense Advanced Research Projects Agency or the U. S. Government.

Rome Air Development Center
Air Force Systems Command
Griffiss Air Force Base, New York

SECRET

Do not return this copy. When not needed, destroy in accordance with pertinent security regulations.

SECRET

SCATTERING MODEL DEVELOPMENT (U)

George D. Thome
B. Rao Pendyala
William H. Russel

Contractor: Raytheon Company
Contract Number: F30602-72-C-0261
Effective Date of Contract: April 1972
Contract Expiration Date: December 1972
Amount of Contract: $50,103.00
Program Code Number: 2E20

Principal Investigator: Dr. George D. Thome
Phone: (617) 443-9521 Ext 3103

Project Engineer: Vincent J. Coyne
Phone (315) 330-3107

Contract Engineer: Richard A. Schneible
Phone: (315) 330-3451

This research was supported by the Defense Advanced Research Projects Agency of the Department of Defense and was monitored by Richard A. Schneible, RADC (OCSE), GAFB, NY 13441 under contact F30602-72-C-0261.

CLASSIFIED BY Proj. Ivy Coral CSG
EXEMPT FROM GENERAL DECLASSIFICATION
SCHEDULE OF EXECUTIVE ORDER 11652
EXEMPTION CATEGORY 3
DECLASSIFY ON 31 December 1982.

SECRET

PUBLICATION REVIEW

This technical report has been reviewed and is approved

RADC Project Engineer

RADC Contract Engineer

FOREWORD (U)

(S) This document contains the written contributions Raytheon has made during 1972 to the development of an RF Scattering Model for the Ivory Coral phenomena. This information is presented in the form of five independent research papers addressing different aspects of the problem. The first three of these papers can also be found in the proceedings of the Prairie Smoke RF-Scattering-Model Workshop[1] and the remaining two will be published in the proceedings of the Prairie Smoke III Data Review Meeting[2]. Such proceedings serve as effective vehicles for getting research results to the modeling segment of the community as soon as possible. However, now that the year's work has been completed, these closely related papers can best be read together and for this reason are being published here as a set.

G. D. Thome

---

1 Proceedings of the Prairie Smoke RF-Scattering-Model Workshop, held at Stanford Research Institute, 18, 19 July 1972.

2 Proceedings of the Prairie Smoke III Data Review Meeting, held at Stanford Research Institute, 31 November - 1 December 1972.

CONTENTS (U)

ASPECT SENSITIVITY - SOME CALCULATIONS AND OBSERVATIONS (U)

G. D. Thome

ASPECT SENSITIVITY: SOME CALCULATIONS AND OBSERVATIONS (U)

by

G. D. Thome

Raytheon Company
Sudbury, Massachusetts

ABSTRACT (U)

(S) In this paper a refined model of the earth's magnetic field is used to compute where in space the RAM radar would see returns from the heated volume over Platteville if the scatterers were strictly field aligned and highly aspect sensitive. These calculations are then compared to the on-frequency target locations measured by RAM on three days and close agreement is found. Backscatter at the transmitted frequency was observed only from those positions in space where the radar looked strictly normal to the magnetic field and this was so even though the true reflection height for the heater frequency on these days was well below (10-30 kilometers) the height where the orthogonality conditions were met. It is concluded that the scatterers responsible for on-frequency RAM backscatter are highly aspect sensitive and are not confined to a small height interval about the heater reflection level. This contrasts with Arecibo results at essentially the same radar frequency in which on-frequency backscatter is observed well off of perpendicularity to the magnetic field (52°) and is observed over only a narrow height interval (less than a kilometer) about the heater reflection level. It appears that RAM and Arecibo are not seeing the same scatterers and this should be borne in mind when the absolute scattering cross-sections from the two sites are compared.

I INTRODUCTION (U)

(S) It has been established that electron density irregularities can be generated by illuminating the ionosphere with intense HF radio waves and that these irregularities are strong enough to support detectable backscatter at HF, VHF and UHF frequencies.[1,2,3] This paper is concerned with the aspect sensitivity of these scatterers at UHF. In particular, attention will be confined to the aspect sensitivity of the on-frequency backscatter observed by the RAM radar at 435 MHz. The intent is to show that on-frequency backscatter is observed at RAM only from those positions within the heated volume where the radar looks strictly perpendicular to the earth's magnetic field. To show this the beam width of the radar must be small compared to the dimensions of the heated volume and this is true only for the UHF frequency at RAM. As of this writing only on-frequency UHF data is available from RAM and consequently no analysis of the off-frequency ("enhanced plasma line") returns is given.

II MAGNETIC FIELD MODEL (U)

(S) The principal components of this analysis are a magnetic field model, a geometrical calculation showing where in space the RAM radar looks normal to the model field, and experimental data showing where in space on-frequency backscatter at 435 MHz has been observed. The model is that of Hendricks and Cain[4] in which the earth's field is represented by a 99-term spherical harmonic fit to surface magnetometer measurements. Since the number of terms in the expansion and the number of magnetometer sites are finite and since the most recent measurements used were taken in 1965, the model is not perfect. A comparison

(S) Cont'd.

between the predicted and the observed field has been made for the Boulder Magnetic Observatory (about 40 km from Platteville). The results are shown below in Table I:

TABLE I. COMPARISON OF PREDICTED AND OBSERVED MAGNETIC FIELD AT THE BOULDER MAGNETIC OBSERVATORY, BOULDER, COLORADO

	PREDICTED	OBSERVED			
			Typical Variations		
	(by Hendricks and Cain)	1971 Average	Quiet Day	Storm	Average Error
Inclination (Dip)	68° 04'	67° 33'	3-6'	10-20'	+31'
Declination	13° 34'	13° 17'	5-10'	20-40'	+17'

Although the average error in inclination and declination is less than a degree, these errors are significantly greater than the irregular variations typical of quiet days. During magnetic storms the field may fluctuate by as much or more than the average model error, but such storms are infrequent (of order once a month). The accuracy of the RAM measurements is such that a half-degree error in the magnetic field model would produce a significant discrepancy between prediction and observation. Consequently a first-order correction has been made to the Hendricks and Cain model by subtracting 31' in inclination angle and 17' in declination angle everywhere in space. This forces the model to correctly predict the average 1971 magnetic field at Boulder. The model is then used to predict the field in the ionosphere above Platteville.

III ASPECT ANGLE CALCULATIONS (U)

(S) The second step in the analysis is to use the corrected magnetic field model and the location of the RAM radar to compute the magnetic aspect angle for points in the vicinity of the heated volume. The radar frequency and the elevation angles of interest are high enough so that refraction can be neglected. Under these conditions the calculation of magnetic aspect angle for a spherical earth can be conveniently done using a geometrical procedure developed by Millman[5] and his approach has been used here. A fixed altitude is chosen, defining a spherical shell around the earth. The magnetic aspect angle from RAM is then computed at closely spaced increments of latitude and longitude and the results plotted on a geographical map of the Platteville area. Contours are drawn showing where the magnetic aspect angle is within 0.1° of 90°. The procedure is repeated for a series of heights and in this way a three-dimensional picture of the 90° magnetic aspect surface in space can be developed. The results are shown in Figure 1. This figure shows that the surface of orthogonality in space for the RAM radar is a dome centered at roughly 43° north latitude, 104° west longitude. The top of the dome is at about 310 km altitude. Over Platteville the surface of the dome is at about 295 km altitude and the surface slopes to the south. A 100 km diameter circle is drawn around Platteville to show about how big the heated volume is in horizontal dimension. The point of this figure is that if the scatterers were highly aspect sensitive, RAM could only detect that fraction of the scatterers lying on the domed surface of orthogonality, no matter how large the disturbed volume actually was. If, for example, scatterers were generated at all altitudes along a 100 km diameter beam above Platteville, RAM would only see those that lay in a thin disk, 100 km in diameter and tilted slightly to the south, with the northernmost edge at about 300 km and the southernmost edge at about 290 km.

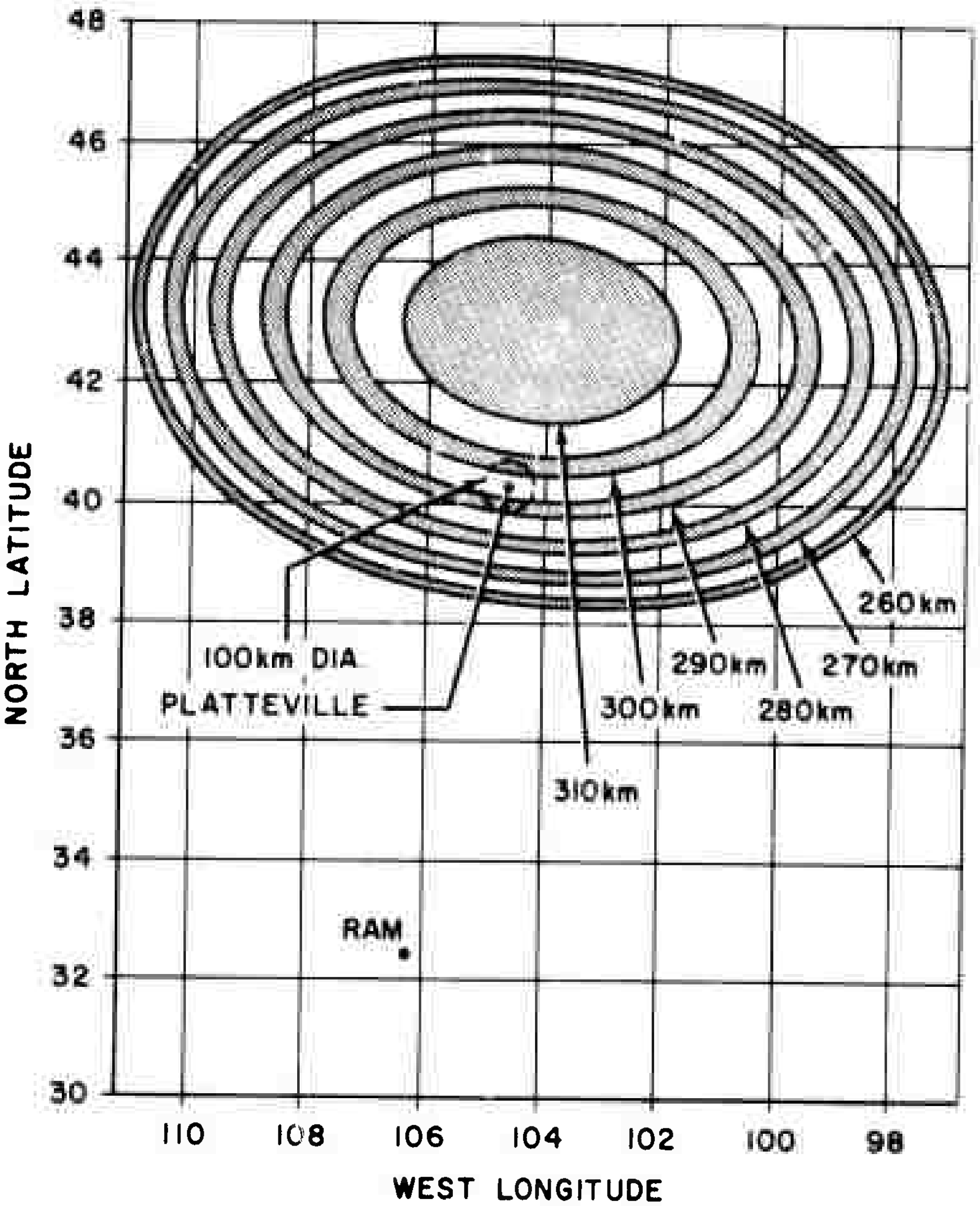

(S) FIGURE 1 POSITIONS IN SPACE AT WHICH THE RAM RADAR CAN LOOK PERPENDICULAR TO THE EARTH'S MAGNETIC FIELD (contours of 90° ± 0.1° magnetic aspect angle as a function of altitude viewed from White Sands) (S)

IV COMPARISONS WITH EXPERIMENTAL DATA (U)

(S) The RAM target location data presented by Minkoff has been plotted in the plane containing RAM, Platteville, and the center of the earth.[2] Figure 2 shows where the domed surface of orthogonality (labeled, "90° magnetic aspect contour") cuts through this plane. If the scatterers were highly aspect sensitive and if the magnetic field model were perfect, RAM targets would appear only along this contour. This figure has been drawn to scale so that RAM data points (given as range, elevation angle pairs) can be plotted directly. Figure 3 is a blow-up of the region above Platteville with several additional pieces of information added. First of all, a stippled band has been added to the 90° magnetic aspect contour showing how far this contour would move due to the 0.1° variation in dip angle typical of magnetically quiet days. This shows that there is about a 5 km uncertainty in the computed position of the 90° contour because of background fluctuations in the magnetic field. RAM target locations for three days have been provided by the Riverside Research Institute[2,6] and are plotted on this figure as circles joined by straight line segments. Data for October 12th, 13th and 14th, 1971 is labeled 12, 13 and 14 respectively. The circles for each day show the southern-most, center and northern-most portions of the target. The accuracy of the target position measurement is set primarily by the accuracy with which the elevation angle of the return can be read from range-time-intensity displays. I estimate that this can be done to an accuracy of about a tenth of the radar beam width and I have made the radius of the circles this size. The third type of data shown on this figure is the true height of the F-region peak at the time the RAM observations were made.[7] These heights are shown as horizontal lines labeled 12, 13 and 14 for October 12, 13 and 14, 1971.

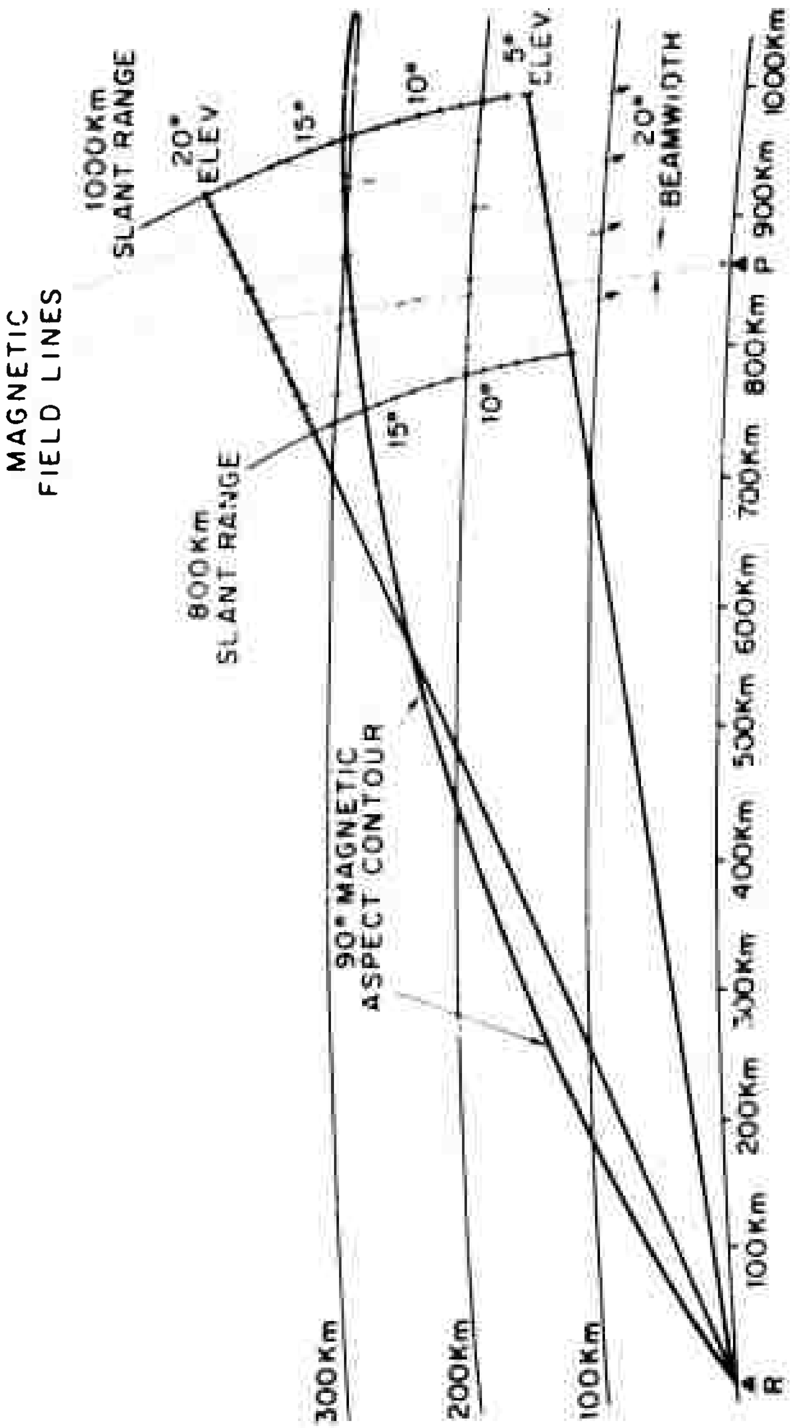

(S) FIGURE 2 SIDE VIEW SHOWING THE GEOMETRY OF THE RAM OBSERVATIONS (U)

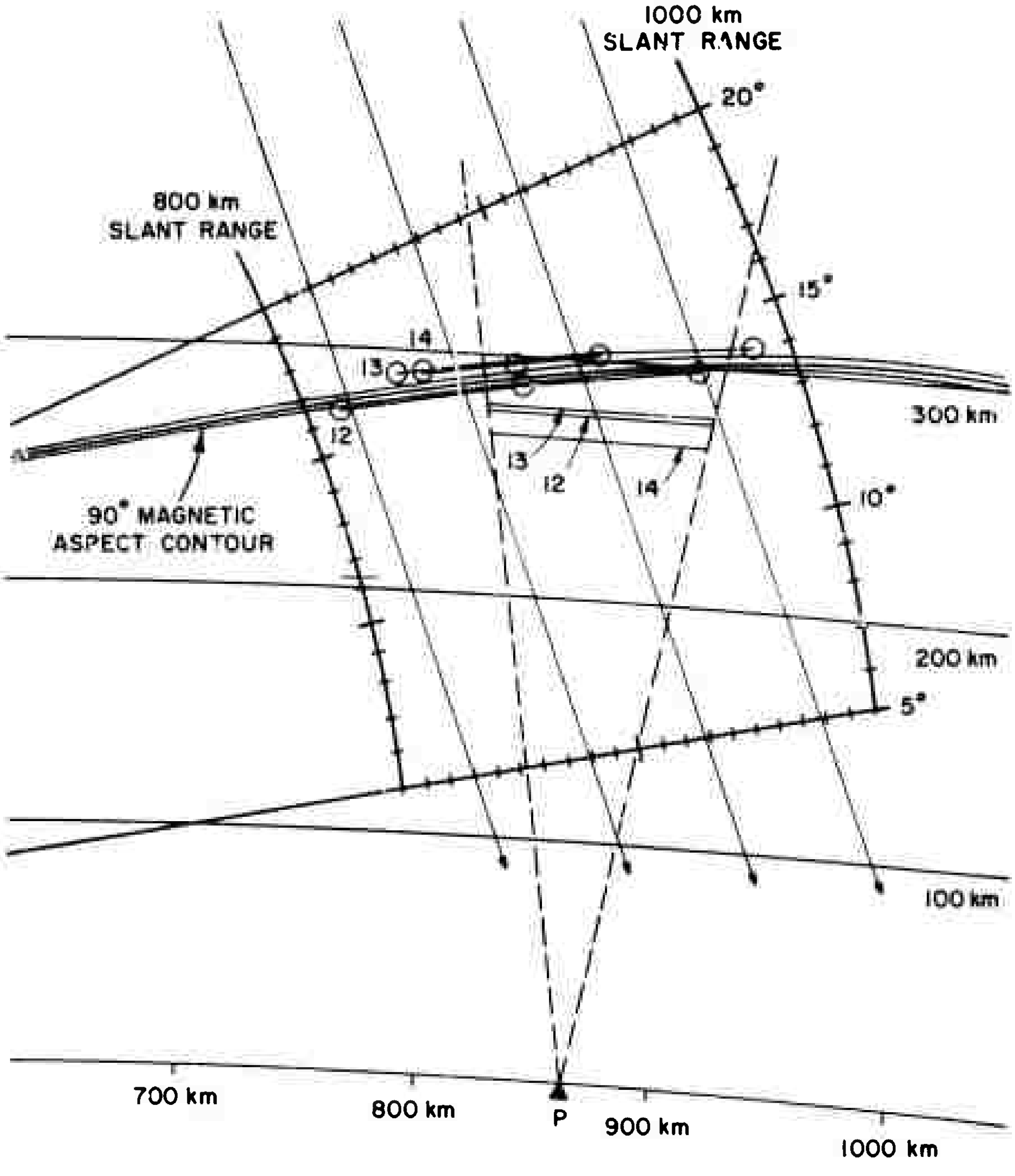

(S) FIGURE 3. EXPANDED DRAWING OF THE EXPERIMENTAL GEOMETRY OVER PLATTEVILLE (U)

(S) The first point to be made from Figure 3 is that the observed returns lie on or very near the 90° contour of orthogonality for RAM suggesting that the scatterers are in fact highly aspect sensitive. By "highly aspect sensitive", I mean that the aspect sensitivity is so great that no echoes can be detected at all unless the radar looks strictly normal to the field. The second point to be made is that the layer peak was well below the altitude where the RAM targets were observed. The reflection height for the heater was presumably at or below the layer peak and consequently it appears that the scatterers responsible for the RAM echoes are well above (by as much as 30 km) the reflection level of the heater. It is suggested that irregularities generated at the heater reflection height are "mapped" up (and presumably down) the field for at least a few tens of kilometers where they can be observed by RAM.

V CONCLUSIONS (U)

(S) Two principal conclusions have been reached:

(S) 1. The scatterers responsible for the RAM on-frequency returns at 435 MHz are highly aspect sensitive, that is, the scatterers must be viewed at 90° to the earth's magnetic field to be detected.

(S) 2. The scatterers are not restricted to a thin disk at the heater reflection height. The RAM echoes usually come from the topside ionosphere whereas the heater reflection level is on the bottomside. It appears that field-aligned irregularities are mapped along the earth's field for at least a few tens of kilometers to a position in space where RAM can view them at normal incidence.

REFERENCES (U)

1. Thome, G.D., and Blood, D.W., "HF Backscatter From White Sands Spread-F Experiment (U)", Raytheon Company, RADC-TR-71-15, 1970, SECRET.

2. Minkoff, J., and Kugelman, P., "Preliminary Summary of Results of Ivory Coral Experiments (U)", Riverside Research Institute, Technical Memorandum TM-38/174-4-50, 1971, SECRET.

3. Fialer, P.A., and Lomasney, J.M., "Prairie Smoke I Sweep-Frequency Backscatter Observations (U)", Stanford Research Institute, in, Proceedings of Prairie Smoke I (U), RF Measurements Data Workshop, 25, 26, 27 January 1972, issued 1972, SECRET.

4. Hendricks, S.J., and Cain, J.C., "Magnetic Field Data for Trapped Particle Evaluations", J. Geophy. Res., Vol. 71, p. 346, 1966, UNCLASSIFIED.

5. Millman, G.H., "Field-Aligned Ionization Scatter Geometry", J. Geophys. Res., Vol. 74, p. 900, 1966, UNCLASSIFIED.

6. Minkoff, J., data exchanged at the Prairie Smoke I Data Workshop, held at Stanford Research Institute, 25-27 January 1972.

7. Utlaut, W., data exchanged at the Prairie Smoke IB Data Workshop, held at Riverside Research Institute, 28-29 March 1972.

AN RF SCATTERING MODEL FOR A RANDOM DISTRIBUTION OF IRREGULARITIES (U)

B. R. Pendyala and G. D. Thome

AN RF SCATTERING MODEL FOR A RANDOM DISTRIBUTION OF IRREGULARITIES (U)

by

B. Rao Pendyala and G. D. Thome

Raytheon Company
Sudbury, Massachusetts

I INTRODUCTION (U)

(U) In 1956 a theory of RF scattering from field aligned irregularities was published by H. G. Booker and applied to the problem of modeling the radar scattering from ionospheric irregularities in the aurora.[1] The starting point for this theory was an ad hoc assumption that electron density irregularities exist in the auroral ionosphere, that these irregularities are randomly distributed in space, and that they exhibit an anisotropic Gaussian autocorrelation function having a greater scale length along the earth's magnetic field than across it. No attempt was made to explain why these irregularities exist or why they are Gaussianly distributed. What was accomplished was to work out the relationship between the physical properties (size, density, anisotropy) of such irregularities and the radar properties. This made it possible to use radar measurements to infer the physical properties of auroral irregularities, it being left to the plasma physicist to explain why irregularities with those properties do in fact exist.

(S) Similarly in this paper, we will use the Booker theory to produce a scattering model for heater generated irregularities. We shall find that

(S) Cont'd.

satisfactory fit to the experimental data can be had assuming that the irregularities are highly aspect sensitive, that their RMS intensity is of the order of 1%, and that their autocorrelation function transverse to the field exhibits two dominant scale sizes, 0.1 meter and 0.5 meter. No attempt is made to reconcile these properties with the plasma physics of the heater-ionosphere interaction because a theory for the generation of such irregularities is not yet available. Until it is, we offer the scattering model described below as a basis for evaluating the usefulness of potential applications, as a guide to the properties the plasma physicists must explain, and as a guide for planning future experiments.

II SCOPE OF THE MODEL (U)

(S) We seek a scattering model which can be used to predict the radar cross-section over bistatic as well as monostatic (backscatter) paths. However, almost all of the quantitative data available for testing the model has been collected over backscatter paths and consequently we shall begin (in Section 3) by deriving a relatively simple model valid for backscatter only. We shall also assume in this initial model that the autocorrelation function of the irregularities, transverse to the magnetic field, is a simple Gaussian. When the predictions of this model are compared (in Section 4) with the experimental data we will find that a significantly better fit to the data can be had by adopting an autocorrelation function which is the sum of two Gaussians of different scale. The scattering model is then rederived for the double Gaussian autocorrelation function and generalized to include the bistatic situation. The

(S) Cont'd.

result, then, is a scattering model which is believed applicable for bistatic as well as for monostatic geometries, which has been validated by comparison with experimental monostatic data, but which has yet to be validated over bistatic paths.

(S) Our model deals only with the on-frequency scatter when the heater is operating at or below f_0f_2 in the ordinary mode with a vertically directed beam. CW heating is assumed with a heater/antenna combination producing the same on-axis density in the ionosphere as does the Platteville heater at full power.

III SCATTERING MODEL (U)

(U) The scattering model presented here is based on the theory of weak scattering (Born approximation) developed by Booker[1] for the case of noniso-tropic Gaussian irregularities. The volume backscattering coefficient derived from the theory is given by Booker as:

$$\sigma_B = (2\pi)^{3/2} \frac{\pi^2}{\lambda_N^4} \left[\frac{\overline{\Delta N}}{N}\right]^2 T^2 L \exp\left\{\frac{-8\pi^2 T^2}{\lambda^2}\right\} \exp\left\{\frac{-8\pi^2}{\lambda^2}(L^2-T^2)\sin^2\psi\right\} \quad (1)$$

The symbols in equation (1) are the same as used by Booker. It is necessary to convert the volume scattering coefficient σ_B to a radar cross-section σ_R as measured by a backscatter system in order to compare the model and the observa-tions.

(U) Let σ_R be the cross section of an equivalent conducting sphere, then the peak backscattered signal power is

$$P_R = \frac{P_{To} G_o^2 \lambda^2 \sigma_R}{(4\pi)^3 R^4} \tag{2}$$

where G_o is the effective on-axis gain (assumed to be the same for transmitting and receiving antennas), P_{To} is the peak power of the transmitted pulse and R is the range to the scattering target. Now consider an elemental volume dv of the scattering target with a scattering coefficient σ_β. Since the isotropic volume scattering coefficient is $4\pi\sigma_\beta$, the received power from the incremental volume will be

$$dP_R = \frac{P_T G^2 \lambda^2 4\pi\sigma_\beta dv}{(4\pi)^3 R^4} \tag{3}$$

Integrating equation (3) over the scattering volume one gets for the total received power

$$P_R = \frac{\lambda^2}{(4\pi)^2 R^4} \int_V P_T G^2 \sigma_\beta dv \tag{4}$$

Equating (2) and (4) leads to

$$\sigma_R = 4\pi \int_V \frac{P_T G^2}{P_{To} G_o^2} \sigma_\beta dv \tag{5}$$

(U) The following assumptions have been made of the scattering volume in order to evaluate the integral in equation (5).

(U) 1. The scattering volume containing field aligned irregularities is cylindrically symmetric about the magnetic field, and is

(U) Cont'd.

centered at a distance D below the point on the field where the radar achieves perpendicularity to the field (Figure 1).

(U) 2. The plasma wavelength, λ_N, is taken as constant with a value corresponding to the specular point. This seems valid since the height interval over which significant scatter comes from is small compared to the scale height of the electron density in the F-region.

(S) 3. $$\overline{(\Delta N/N)^2} = \overline{(\Delta N/N)_0^2} \exp\left\{-\left[\frac{x^2}{w^2} + \frac{y^2}{w^2} + \frac{(z+D)^2}{H^2}\right]\right\}$$

$\overline{(\Delta N/N)^2}$ varies with x and y because the heater beam is of finite width and varies with z since the irregularities weaken as one moves above or below the heater reflection level. Since the interval in z over which significant scatter comes is small compared to H, it is only the value of $\overline{(\Delta N/N)^2}$ at z=0 which counts, so we can write

$$\overline{(\Delta N/N)^2} = \overline{(\Delta N/N)_0^2} \exp\left\{-D^2/H^2\right\} \exp\left\{-\left[\frac{x^2+y^2}{w^2}\right]\right\}$$

where $\overline{(\Delta N/N)_0^2}$ is the peak value of $\overline{(\Delta N/N)^2}$ which occurs at the heater reflection level.

(U) 4. $\sin^2\psi = z^2/R^2$ since significant scatter obtains only for small values of z/R, i.e., near specularity.

(U) 5. The antenna has a Gaussian beam of half-width B radians so that

$$G = G_0 \exp\left\{-\left[\frac{y^2+z^2}{(BR)^2}\right]\right\}$$

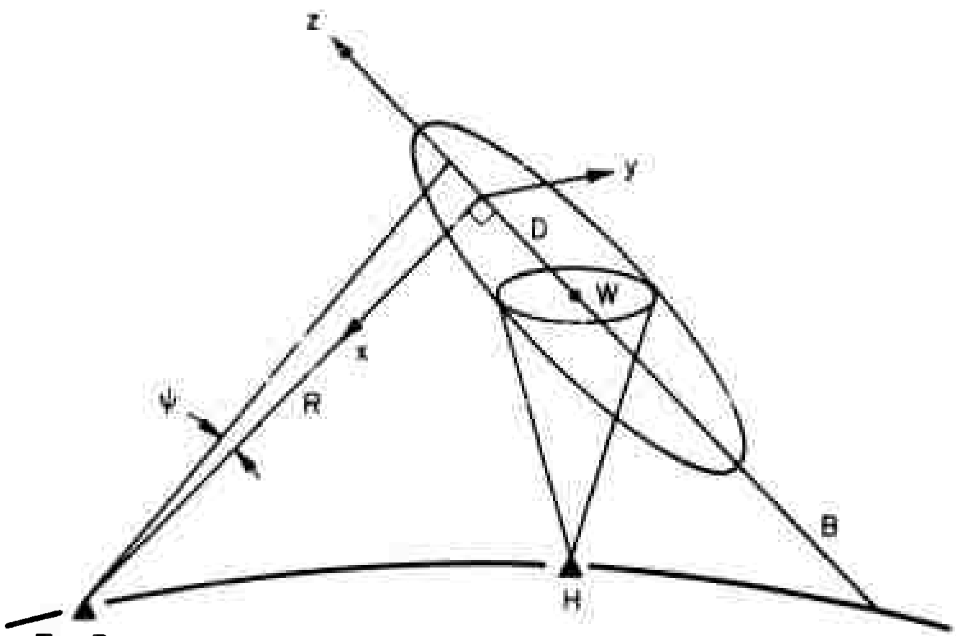

(S) FIGURE 1. BACKSCATTER GEOMETRY FOR THE HEATER DIAGNOSTIC RADAR (S)

(U) Cont'd.

The transmitted pulse has a Gaussian half-width P so that

$$P_T = P_{To} \exp\left\{-(x^2/P^2)\right\}$$

(U) On incorporating the above assumptions, the volume integral in equation (5) becomes:

$$\sigma_R = 4\pi \int_V \left[\exp\left\{-\left[\frac{x^2}{P^2} + \frac{2y^2}{(BR)^2} + \frac{2z^2}{(BR)^2}\right]\right\}\right] (2\pi)^{3/2} \frac{\pi^2}{\lambda_N^4} \cdot$$

$$\overline{\left[\frac{\Delta N}{N}\right]_o^2} \exp\left\{-D^2/H^2\right\} \exp\left\{-\frac{(x^2+y^2)}{w^2}\right\} T^2L \exp\left\{\frac{-8\pi^2T^2}{\lambda^2}\right\} \cdot$$

$$\exp\left\{-\frac{8\pi^2(L^2 - T^2)\, z^2}{\lambda^2R^2}\right\} dv$$

Let dv = dx dy dz and integrate over all space:

$$\sigma_R = \frac{8\pi^4\sqrt{2\pi}}{\lambda_N^4} \left[\frac{\Delta N}{N}\right]_o^2 T^2L \exp(-D^2/H^2) \exp\left\{-\frac{8\pi^2T^2}{\lambda^2}\right\} \cdot$$

$$\int_{-\infty}^{\infty} \exp\left\{-\left(\frac{1}{P^2} + \frac{1}{w^2}\right)x^2\right\} dx \cdot \int_{-\infty}^{\infty} \exp\left\{-\left(\frac{2}{(BR)^2} + \frac{1}{w^2}\right)y^2\right\} dy \cdot$$

$$\int_{-\infty}^{\infty} \exp\left\{-\left(\frac{2}{(BR)^2} + \frac{8\pi^2}{\lambda^2}\,\frac{(L^2 - T^2)}{R^2}\right) z^2\right\} dz$$

(U) Cont'd.

The integrals are all of the form $\int_{-\infty}^{\infty} e^{-a^2x^2}\,dx$ so that

$$\sigma_R = \frac{8\pi^4}{\lambda_N^4}\sqrt{2\pi}\,\overline{(\Delta N/N)_o^2}\;T^2L\;\exp\left\{-D^2/H^2\right\}\;\exp\left\{\frac{-8\pi^2T^2}{\lambda^2}\right\}$$

$$\frac{\sqrt{\pi}}{\left[\frac{1}{P^2}+\frac{1}{W^2}\right]^{1/2}}\;\frac{\sqrt{\pi}}{\left[\frac{2}{(BR)^2}+\frac{1}{W^2}\right]^{1/2}}\;\frac{\sqrt{\pi}}{\left[\frac{2}{(BR)^2}+\frac{8\pi^2(L^2-T^2)}{\lambda^2R^2}\right]^{1/2}}$$

Since L>>T for high aspect sensitivity, the last square root term may be simplified to

$$\left[\frac{2}{(BR)^2}+\frac{8\pi^2L^2}{\lambda^2R^2}\right]^{1/2} = \frac{2\sqrt{2}\pi L}{\lambda R}\left[1+\frac{\lambda^2}{4\pi^2L^2B^2}\right]^{1/2}$$

The second term in the root is much less than 1 which means that it is the aspect sensitivity which sets the vertical thickness of the effective scattering volume rather than the vertical beam width of the antenna. Hence,

$$\sigma_R = \frac{4\pi^5W^2RT^2\lambda}{\left[1+(W/P)^2\right]^{1/2}\left[1+2(W/BR)^2\right]^{1/2}}\;\frac{\overline{(\Delta N/N)_o^2}}{\lambda_N^4}\;\exp\left\{-D^2/H^2\right\}\exp\left\{\frac{-8\pi^2T^2}{\lambda^2}\right\} \qquad (6)$$

(S) Equation (6) can be used to predict the backscatter cross section in terms of

- P, the Gaussian radius of the pulse
- B, the Gaussian radius of the antenna beam
- R, the range from radar to the specular point in the scattering volume
- T, the Gaussian autocorrelation distance for density fluctuations transverse to the magnetic field

(S) Cont'd.

λ, the operating wavelength

D, the separation along the field between the specular point and the heater reflection level

H, the e-folding distance for the variation of $\overline{(\Delta N/N)^2}$ along z

$\overline{(\Delta N/N)^2}$, the mean square electron density fluctuations of the irregularities

λ_N, the plasma wavelength corresponding to the ambient plasma frequency at the specular point

W, the Gaussian radius of the heated volume in a horizontal plane at the reflection level

The parameters P and B are related to the commonly expressed half-power beam width and pulse length as

$$B = 0.60 \text{ (HPBW)} \quad \text{and} \quad P = 0.564\ (c\tau/2)$$

(S) The measured radar cross section σ_R corresponds to a scattering volume which in general represents only a fraction of the total volume of the heater generated irregularities. In a situation where (W/P) and (W/BR) are much less than unity which means that the radar pulse encompasses the entire volume of the irregularities, the measured cross section stands for the total cross section of the disturbance and it is given as:

$$\sigma_T = 4\pi^5 W^2 R T^2 \lambda \frac{\overline{(\Delta N/N)_o^2}}{\lambda_N^4} \exp\left\{-D^2/H^2\right\} \exp\left\{\frac{-8\pi^2 T^2}{\lambda^2}\right\}$$

The radar cross section measurements reported by Fialer, Evans and Lomasney[2] using SRI SFCW sounder observations are in the form of σ_T. The VHF and UHF

(S) Cont'd.

cross sections obtained from RAM radar observations reported by Minkoff[3,4,5] which represent σ_R have been converted to σ_T to standardize with the SRI measurements, facilitating an easy comparison with the scattering model.

IV COMPARISON BETWEEN MODEL AND OBSERVATIONS (U)

IV.A Single Gaussian Scale Size (U):

(S) Using the equation (7) which is appropriate to a single Gaussian scale size, the total scattering cross section is computed as function of frequency in the range 10-435 MHz for different values of T. The values adopted for the various parameters are as follows:

$$W = 90 \text{ km}$$
$$R = 900 \text{ km}$$
$$\lambda_N = 54 \text{ m}$$
$$D = 0$$

The value of $\overline{(\Delta N/N)^2}$ is adjusted in each case so that the computed cross section matches the observed at the low frequency end. Figure 2 presents a comparison between the observations and the curves based on the scattering model. The curves shown are parametric in T in the range 0.1 to 1.0 m. The required values for $(\Delta N/N)_{RMS}$ fall in the range 0.3 to 7% with higher values going with lower T. The curve for T = 0.1 m estimates cross sections well above the observed for VHF and UHF whereas T = 1.0 m provide at the other extreme cross sections far below the observed values. The curve for T = 0.3 m seems to be the closest fit to the observations of all the four curves presented.

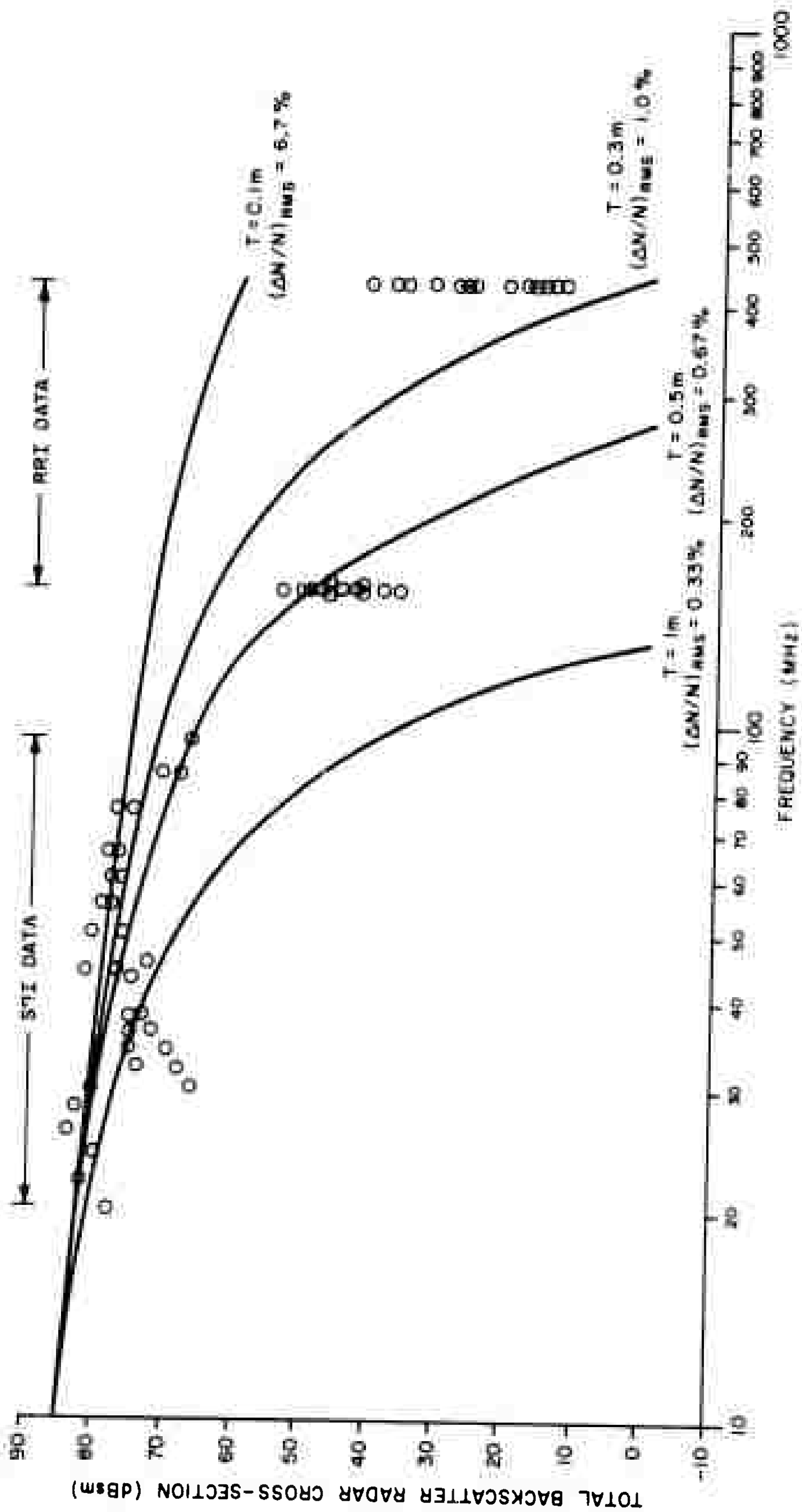

(S) FIGURE 2. A COMPARISON BETWEEN THE OBSERVATIONS AND A MODEL BASED ON GAUSSIAN IRREGULARITIES (S)

(S) Cont'd.

It should, however, be clear from the comparison that the shape of the computed curve is such that no single scale size can satisfactorily reproduce the observed frequency dependence of the cross section. It is, therefore, attempted, in the section to follow, to explain the observations on the basis of a two scale size model.

IV.B <u>Sum of Two Gaussian Scale Sizes (U)</u>:

(U) We shall treat in this section the presence of two Gaussian scale sizes, first for the general case of bistatic configuration and then reduce the equations to the backscatter case of present interest. The volume scattering coefficient for a bistatic case is expressed as:

$$\sigma_v = \overline{\left|\Delta\varepsilon/\varepsilon\right|^2} \frac{\pi^2 \sin^2 x}{\lambda^4} P \left\{K(\ell_2-\ell_1),\ K(m_2-m_1),\ K(n_2-n_1)\right\} \quad (8)$$

where P is the power spectrum of $(\Delta\varepsilon/\varepsilon)$

Let us assume that the autocorrelation function of $\Delta\varepsilon/\varepsilon$ is a sum of two Gaussian functions with different scale sizes, i.e.,

$$P(x,y,z) = \alpha \exp\left\{-1/2\left[\frac{(x^2+y^2)}{T_1^2} + \frac{z^2}{L_1^2}\right]\right\} + (1-\alpha)\exp\left\{-1/2\left[\frac{(x^2+y^2)}{T_2^2} + \frac{z^2}{L_2^2}\right]\right\} \quad (9)$$

Fourier transform of the above equation gives

$$P(\xi,\eta,\zeta) = (2\pi)^{3/2}\left\{\alpha T_1^2 L_1 \exp\left[-1/2\left\{T_1^2(\xi^2+\eta^2)+L_1^2\zeta^2\right\}\right]\right.$$
$$\left. + (1-\alpha) T_2^2 L_2 \exp\left[-1/2\left\{T_2^2(\xi^2+\eta^2)+L_2^2\zeta^2\right\}\right]\right\} \quad (10)$$

(U) Cont'd.

Set $\xi = K(\ell_2-\ell_1)$, $\eta = K(m_2-m_1)$ and $\zeta = K(n_2-n_1)$

and substitute $\overline{|\Delta\varepsilon/\varepsilon|^2} = (\lambda/\lambda_N)^4\ \overline{(\Delta N/N)^2}$ to obtain

$$\sigma_V = (2\pi)^{3/2}\ \pi^2 \sin^2 x \frac{\overline{(\Delta N/N)^2}}{\lambda_N^4} \Big\{ \alpha T_1^2 L_1 \exp\Big[-1/2 \big\{ K^2T_1^2(\ell_2-\ell_1)^2$$

$$+ K^2T_1^2\ (m_2-m_1)^2 + K^2L_1^2\ (n_2-n_1)^2\big\}\Big] + (1-\alpha)\ T_2^2L_2$$

$$\exp\Big[-1/2\big\{K^2T_2^2(\ell_2-\ell_1)^2 + K^2T_2^2\ (m_2-m_1)^2 + K^2L_2^2\ (n_2-n_1)^2\big\}\Big]\Big\} \quad (11)$$

Let us define a coordinate system centered at the scattering volume with z axis along the magnetic field and y axis along the magnetic east as shown in Figure 3. The locations of the transmitter and receiver be (x_1, y_1, z_1) and (x_2, y_2, z_2) respectively. Now consider a unit scattering volume in the disturbance whose coordinates are (x, y, z). Then we have for the direction cosines

$$\ell_1 = \frac{(x - x_1)}{R_1}, \qquad m_1 = \frac{(y - y_1)}{R_1}, \qquad n_1 = \frac{(z - z_1)}{R_1}$$

and

$$\ell_2 = \frac{(x_2 - x)}{R_2}, \qquad m_2 = \frac{(y_2 - y)}{R_2}, \qquad n_2 = \frac{(z_2 - z)}{R_2}$$

where R_1 and R_2 are the ranges from the transmitter and the receiver to the scattering volume.

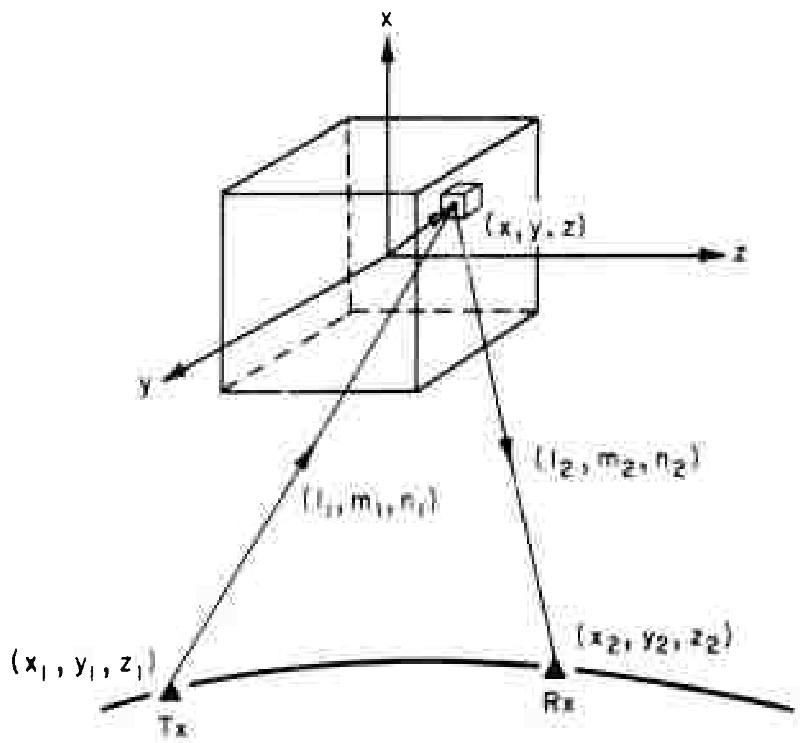

(U) FIGURE 3. SCATTERING GEOMETRY FOR BISTATIC CONFIGURATION (U)

(U) Cont'd.

Let us denote

$$(\ell_2-\ell_1)^2 = \left[\frac{x_1}{R_1} + \frac{x_2}{R_2} - x\left(\frac{1}{R_2} + \frac{1}{R_1}\right)\right] = \left[A_1 + Bx\right]^2$$

$$(m_2-m_1)^2 = \left[A_2 + By\right]^2 \qquad (12)$$

$$(n_2-n_1)^2 = \left[A_3 + Bz\right]^2$$

where A_1, A_2, A_3 and B are all constants.

Substitute (12) in equation (11) and integrate over all space to get

$$\sigma_{RB} = 4\pi \int_{-\infty}^{\infty}\int_{-\infty}^{\infty}\int_{-\infty}^{\infty} \frac{P_T}{P_{To}} \frac{G(\ell_1,m_1,n_1)\ G(-\ell_2,-m_2,-n_2)}{G_0^2} \sigma_V dx\ dy\ dz \qquad (13)$$

In the above equation the transmitting and receiving antennas are assumed to have identical gain patterns. The magnetic aspect in a bistatic configuration is given from the direction of the bisector of the incident and scatter directions. The angle ψ which is the complement of the angle between the bisector and the magnetic field is given by the relation

$$\sin\psi = (n_2-n_1)/\left[(\ell_2-\ell_1)^2 + (m_2-m_1)^2 + (n_2-n_1)^2\right]^{1/2} \qquad (14)$$

For the backscatter case of present interest, we substitute

$$(\ell_1,m_1,n_1) = -(\ell_2,m_2,n_2) = (\ell,m,n)$$

$n^2 = \sin^2\psi$ and $(\ell^2+m^2) = \cos^2\psi$ to get

(U) Cont'd.

$$\sigma_\beta = (2\pi)^{3/2}\pi^2\overline{(\Delta N/N)^2}\left\{\alpha T_1^2 L_1 \exp\left[\frac{-8\pi^2 T_1^2}{\lambda^2}\right]\exp\left[\frac{-8\pi^2}{\lambda^2}(L_1^2-T_1^2)\sin^2\psi\right]\right.$$

$$\left. + (1-\alpha)\, T_2^2 L_2 \exp\left[\frac{-8\pi^2 T_2^2}{\lambda^2}\right]\exp\left[\frac{-8\pi^2}{\lambda^2}(L_2^2-T_2^2)\sin^2\psi\right]\right\} \quad (15)$$

(S) Following the steps described in Section 3, the total cross section is given as:

$$\sigma_T = \frac{4\pi^5 w^2 R\lambda\ \overline{(\Delta N/N)_0^2}}{\lambda_N^4}\exp\left\{-D^2/H^2\right\}\left\{\alpha T_1^2 \exp\left[\frac{-8\pi^2 T_1^2}{\lambda^2}\right] + (1-\alpha) T_2^2 \exp\left[\frac{-8\pi^2 T_2^2}{\lambda^2}\right]\right\} \quad (16)$$

From equation (16) it should be obvious that any number of scale sizes can be added without altering the form of the equation. Judging from the results presented in Figure 2, it seems that a combination of the scale sizes with T=0.1 and 0.5 m is best suited to obtain a reasonable fit to the experimental measurements. Figure 4 shows a fit of the two scale size model with the measurements, and in addition curves are presented there also for individual scale sizes for comparison. A value of about 0.8% for $(\Delta N/N)_{RMS}$ with the larger irregularities nearly twice as strong as the smaller was found necessary to obtain a match between the model and the observations. The comparison shown here makes it clear that it is essential to allow more than single scale size to exist in the scattering volume in order that the model predicts the same shape as the observations seem to indicate for the frequency dependence of the scattering cross section.

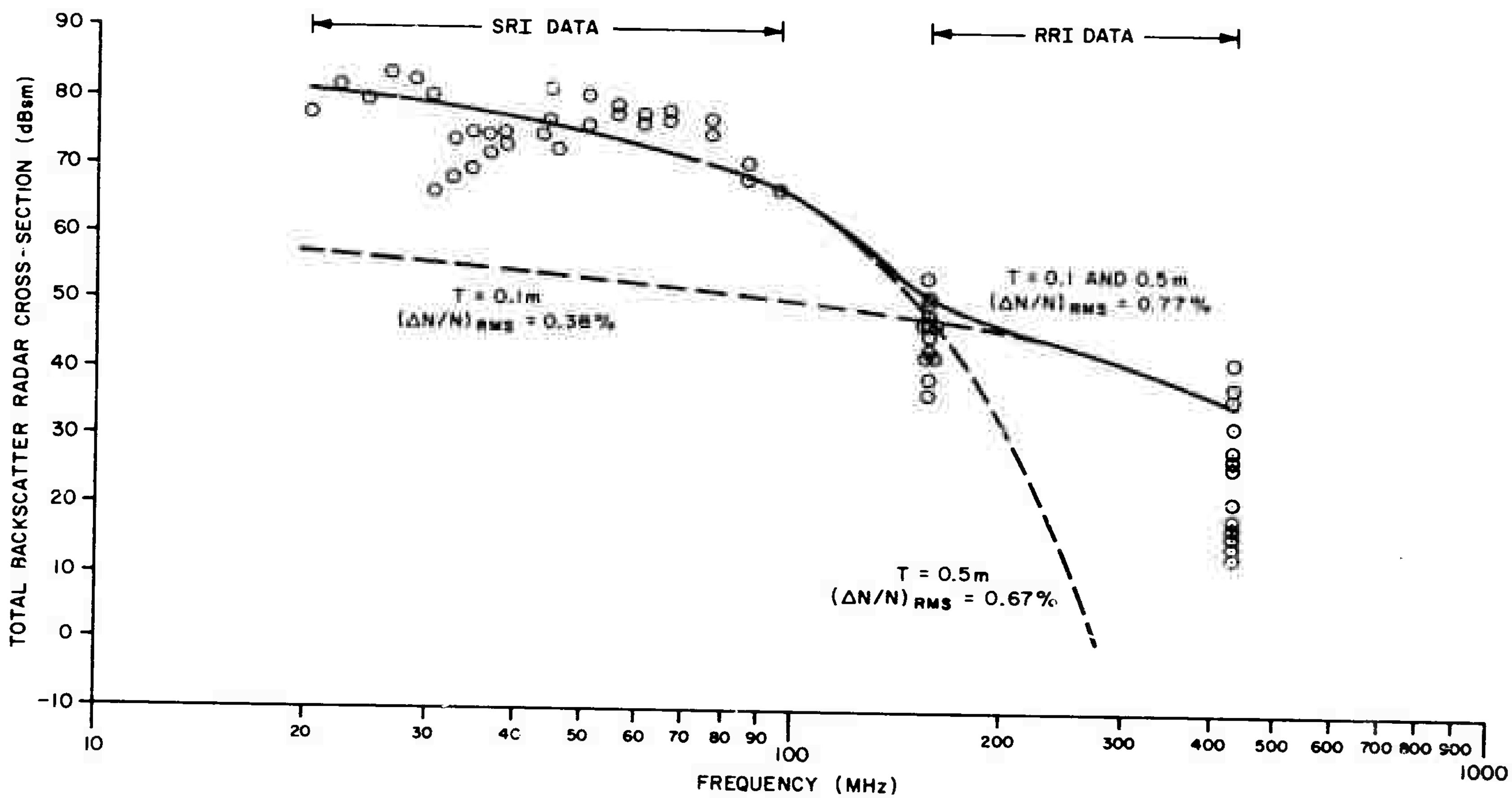

(S) FIGURE 4. A FIT OF THE TWO-SCALE-SIZE SCATTERING MODEL TO THE OBSERVATIONS (S)

REFERENCES (U)

1. Booker, H.G., "A Theory of Scattering by Nonisotropic Irregularities with Application to Radar Reflections from the Aurora" (U), J.A.T.P., Vol. 8, pp 204-221, 1956, UNCLASSIFIED.

2. Fialer, P.A., P.C. Evans and L.M. Lomasney, Prairie Smoke I: Sweep-Frequency Backscatter Observations (U), S.R.I. Technical Report 13, March 1972, SECRET.

3. Minkoff, J. and P. Kugelman, Preliminary Summary of Results of Ivory Coral Experiments (U), R.R.I. Technical Memorandum TM-38/174-4-50, 29 December 1971, SECRET.

4. Minkoff, J., P. Kugelman and M. Laviola, "Preliminary Summary of Results of Prairie Smoke IB Experiments (U)", R.R.I. Research Memorandum M-1/174-4-50, 1 March 1972, SECRET.

5. Minkoff, J., P. Kugelman and M. Laviola, "Preliminary Summary of Results of Prairie Smoke II Experiments (U)", R.R.I. Research Memorandum M-2/174-4-50, 1 June 1972, SECRET.

RF SCATTERING MODEL SUMMARY
JULY 1972 (U)

G. D. Thome

RF SCATTERING MODEL SUMMARY: JULY 1972 (U)

by

G. D. Thome

Raytheon Company
Sudbury, Massachusetts

ABSTRACT

(S) On July 18-19, 1972 an RF Scattering Model Workshop was held at the Stanford Research Institute in California. The purpose of this workshop was to arrive at a model of the scattering phenomenon which is consistent with existing experimental data, which can be used to predict the performance of hypothetical scatter communication systems, and which will serve as a focal point for planning future theoretical and experimental efforts in this area. We have produced such a model and we present it here for use by the community. This model should be viewed as a statement of the present state-of-the-art rather than a finished product.

I INTRODUCTION (U)

(S) The model is intended primarily for use in predicting the performance of communication systems using the Ivory Coral scattering phenomenon. Ideally the model would be derived directly from a plasma physics theory of the heater-ionosphere interaction and would be generally applicable to all scattering situations of practical interest. It will probably be at least a year before the relevant theory is developed to the point where this can be done. At the other extreme, the model could be given simply as a tabulation of experimental results. The problem with this approach is that data is available over only a limited number of paths and with only a few types of equipment. A tabulation of experimental results provides no information about how to extrapolate these results to other situations. As an interim solution we have divided the modeling task into three parts,

1. on-frequency scattering
2. plasma line scattering
3. scintillation

The on-frequency scattering and scintillation will be handled by asking what size, shape and distribution of heater-produced ionospheric irregularities will scatter in the observed way. Given these irregularities, the on-frequency scatter and the scintillation under other experimental conditions can be predicted. The theory for plasma line scattering is far enough along so that in this case a satisfactory scattering model can be derived directly from the theory. This paper is devoted essentially to the on-frequency scattering model while the models for the latter two were presented by Perkins[1] and Bowhill[2], respectively.

II PHYSICAL DESCRIPTION (U)

(S) The model has been developed for the Platteville transmitter heating at full power with ordinary ray polarization and with a vertically directed beam. The heater frequency is assumed to be at or below the critical frequency of the ionosphere. A sketch of the disturbed volume which develops under these situations is shown in Figure 1. For the sake of clarity, the heater beam has been idealized as having sharp edges, that is, the gain is constant within the beam but drops abruptly to zero outside of the beam. The heating wave reflects at the altitude where the heater frequency equals the local plasma frequency. The irregularities responsible for plasma line scatter are generated at essentially this same altitude and are confined there. These irregularities are not extremely aspect sensitive and consequently to a radar the plasma line scatter appears to come from a thin disk which can be moved up or down in altitude by changing the heater frequency. A second group of irregularities are also generated at the heater reflection height and these are responsible for on-frequency scattering. In contrast to the plasma-line irregularities (which are probably caused by propagating waves) the on-frequency irregularities are essentially stationary in space and extend along the earth's magnetic field for several tens of kilometers. The on-frequency irregularities are highly aspect sensitive and consequently scatter significantly only when specularity is achieved. For the backscatter case shown in Figure 1, this means that the radar must look perpendicular to the magnetic field in order to detect a signal. The locus of points for which the radar can look perpendicular to the field is called the orthogonality contour and this is fixed in space by geography alone, having nothing to do with the heater parameters. The

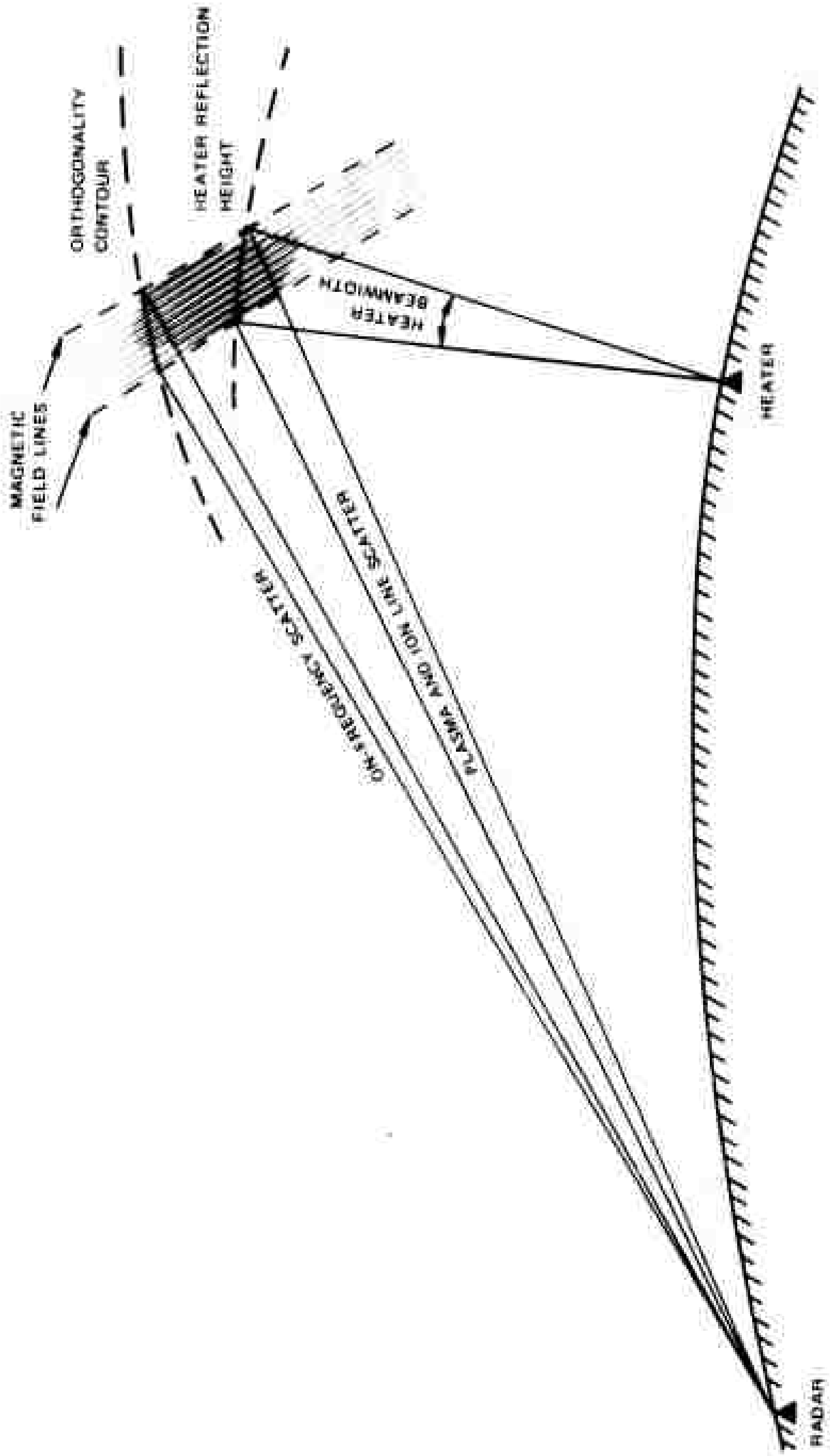

(S) FIGURE 1 SKETCH OF THE RF SCATTERING MODEL (U)

(S) Cont'd.

on-frequency irregularities are most intense at the heater reflection height and consequently the strongest on-frequency scatter will be observed when the heater reflection level is adjusted to coincide with the orthogonality contour.

III ON-FREQUENCY SCATTERING MODEL (U)

(S) The on-frequency scattering model has been arrived at by applying the Booker theory[3] for scattering from anisotropic irregularities to the Ivory Coral problem. Booker applied his theory to the problem of radio wave scattering from the aurora and found that the experimental data could be understood if there were weak irregularities of electron density present that were aligned with the earth's magnetic field. We find the same to be true for the heated volume over Platteville. As with the auroral case, there is no attempt made to explain how these irregularities are produced or maintained. This is a plasma physics question and is being addressed by the Ivory Coral theorists at the present time.

(S) The scattering model we present is a volume scattering coefficient which must be integrated over the heated volume to give the total power received over a given path. Several alternatives exist for doing the required integration in practice. For special cases the integration can be done analytically leading to simple formulas which can be evaluated on a slide rule. For example, this has been done for the case of backscatter measurements made magnetically south of the heated volume (the situation under which most of our experimental data was taken) and this has simplified the task of varying the parameters of the model to fit the backscatter (or near backscatter) observations.

(S) Cont'd.

It is likely that satisfactory analytic integrations can be done for most specific cases of interest but these must be looked at one at a time to decide what idealizations are appropriate. The more general approach is to use a computer to numerically integrate the volume scattering coefficient over the heated volume. In this way realistic antenna patterns, magnetic field models, and ambient electron density profiles can be used. If this approach is followed it will probably be important to minimize the computer time required. One promising way of doing this is to recognize that the high aspect sensitivity of the scatterers means that only that fraction of the heated volume that lies near the specularity surface for the communications link being studied need be considered in the integral. In other words, the volume integral can be reduced to a surface integral[4] with an appreciable saving in computer time.

(U) The volume scattering coefficient (power scattered in the direction of the receiver, per unit solid angle, per unit incident power density, per unit volume) is[5]

$$\sigma_V = (2\pi)^{3/2}\,\pi^2 \sin^2\chi \,\frac{\overline{(\Delta N/N)^2}}{\lambda_N^4}\left\{ \alpha T_1^2 L_1 \left[\exp - \frac{8\pi^2 \sin^2\frac{\theta}{2}}{\lambda^2}\left(T_1^2\cos^2\psi + L_1^2\sin^2\psi\right)\right] + (1-\alpha) T_2^2 L_2 \left[\exp - \frac{8\pi^2 \sin^2\frac{\theta}{2}}{\lambda^2}\left(T_2^2\cos^2\psi + L_2^2\sin^2\psi\right)\right]\right\} \quad (1)$$

where

χ = angle between the direction of scattering and the electric field of the incident wave

θ = angle between the incident and scattered wave directions

(U) Cont'd.

ψ = complement of the angle between the external bisector to incident and scattered directions and the magnetic field

λ = operating wavelength

λ_N = the plasma wavelength corresponding to the ambient electron density

$\overline{(\Delta N/N)^2}$ = the mean square electron density fluctuations of the irregularities

T_1, T_2 = Gaussian autocorrelation scale sizes for density fluctuations transverse to the magnetic field

L_1, L_2 = Gaussian autocorrelation scale sizes for density fluctuations parallel to the magnetic field

α = a constant determining the relative strength of the two Gaussian irregularity distributions used in this model

(U) There are three angles involved in the model; χ, θ, and ψ. The angle χ accounts for the fact that the irregularities scatter much like small dipoles with the null direction along the E field of the incident wave. The term $\sin^2\chi$ can be made unity by suitable choice of transmitter and receiver polarizations. The angles θ and ψ are illustrated in Figure 2. Let the scattering plane be defined by the transmitter, the scattering volume element, and the receiver. Since this is weak scattering, most of the incident signal continues on through the scattering volume without deviation and this is called the transmitted signal. The angle between the transmitted and the scattered signal is defined as θ. The bisector of the path from transmitter to scattering volume to receiver also lies in the scattering plane. The angle between this bisector and the magnetic field is defined as $(90 - \psi)°$.

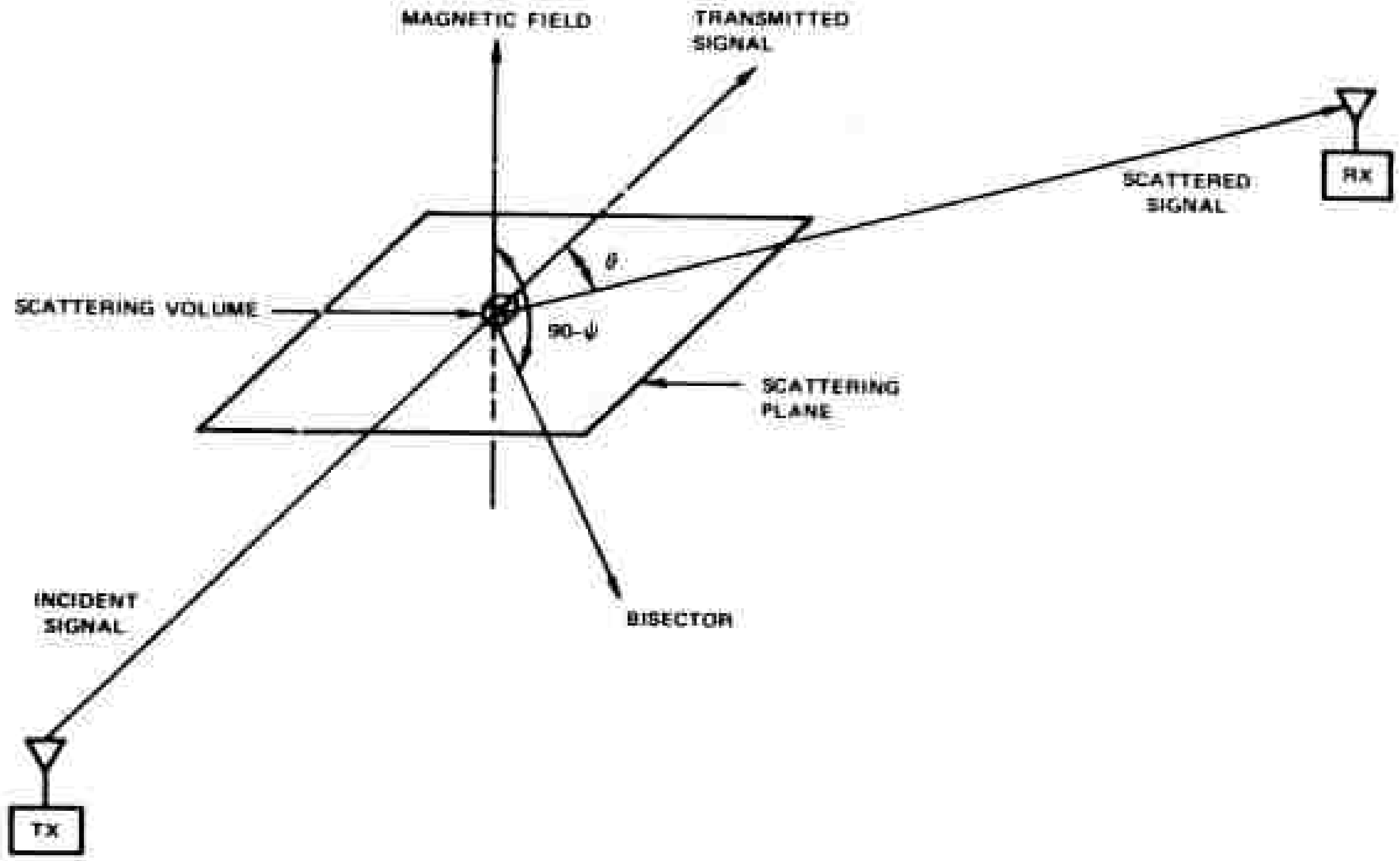

(S) FIGURE 2 BISTATIC SCATTERING GEOMETRY (U)

(S) The operating wavelength of the communication system is λ. The local electron density is given in terms of the wavelength, λ_N, corresponding to the local plasma frequency. λ_N will vary through the heated volume and should be included in the volume integration.

(S) The intensity of the electron density fluctuations is given by $\overline{(\Delta N/N)^2}$ and this varies throughout the heated volume. The maximum value, $\overline{(\Delta N/N)}_0^2$, occurs at the heater reflection level on the axis of the heater beam. At points off the axis of the heater beam but still at the heater reflection level, $\overline{(\Delta N/N)^2}$ is proportional to the heater power density. Thus for a Gaussian heater beam, $\overline{(\Delta N/N)^2}$ varies in a Gaussian manner across the heater reflection plane. The strength of the irregularities drops off above and below the heater reflection level with a Gaussian scale height A. This aspect of the model is illustrated in Figure 3.

(S) In the Booker auroral scattering model the characteristics of the irregularities are specified by a two-dimensional autocorrelation function having a correlation length T transverse to the earth's magnetic field and a correlation length L along the field. Essentially, T controls the frequency dependence and L/T controls the aspect sensitivity of the scatterers. In order to match the frequency dependence observed in the Ivory Coral phenomenon we must assume that two sets of irregularities are present, one set with a transverse correlation distance T_1 and another with a transverse correlation distance T_2. The experimental measurements to date give no evidence for aspect sensitivity less than perfect. That is, there is no reason to assume a finite L and the model could be simplified somewhat by using a one-dimensional auto-correlation function (variations across the field only). However, the

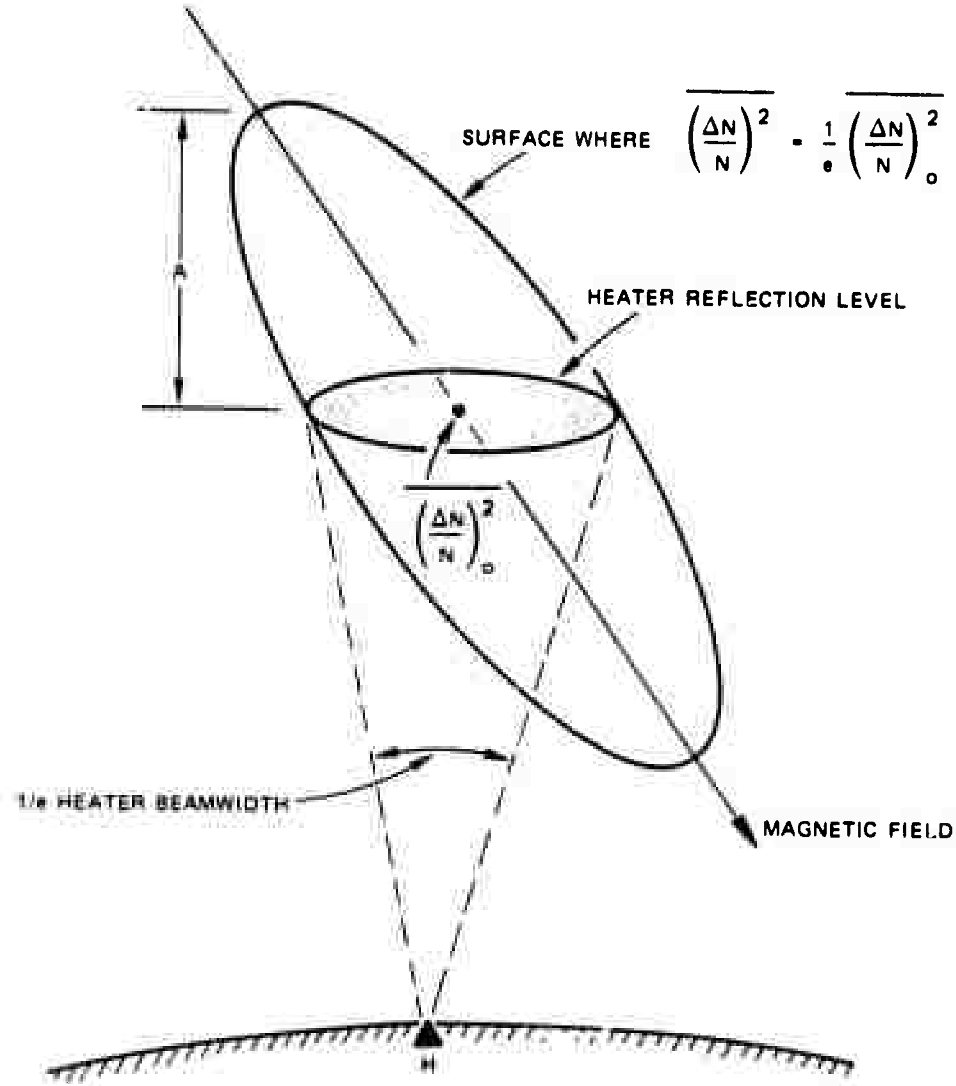

(S) FIGURE 3 SPATIAL VARIATION OF $\overline{(\Delta N/N)^2}$ (U)

(S) Cont'd.

simplification is not great and aspect sensitivity experiments are still underway (HF-VHF interferometry) so for the present we shall retain the parameter L in the model and assign it a large enough numerical value to produce high aspect sensitivity. The relative strength of the two sets of Gaussian irregularities in this model is set by the parameter α .

(S) The constants $\overline{(\Delta N/N)_0^2}$, A, T_1, T_2, L_1, L_2 and have been evaluated from the available experimental data and found to be the following:

$$\overline{(\Delta N/N)_0^2} = 0.6 \times 10^{-4}$$

$$A = 10 \text{ kilometers}$$

$$T_1 = 0.1 \text{ meter}$$

$$T_2 = 0.5 \text{ meters}$$

$$L_1 = L_2 = 10 \text{ kilometers}$$

$$\alpha = 0.24$$

The bulk of the quantitative experimental data in the Ivory Coral program has been collected over backscatter paths or over bistatic paths which are so close to the backscatter geometry that the difference is insignificant. These experimental results are summarized by the shaded band (1) shown in Figure 4. The computed backscatter curve using the on-frequency scattering model with the constants given above is shown by the solid curve labeled (2). The model prediction is seen to match the experimental measurements to within the uncertainty of the data. The solid curve labeled (3) on this figure is the model prediction over a bistatic path for which the scattering angle is 60°. The important point

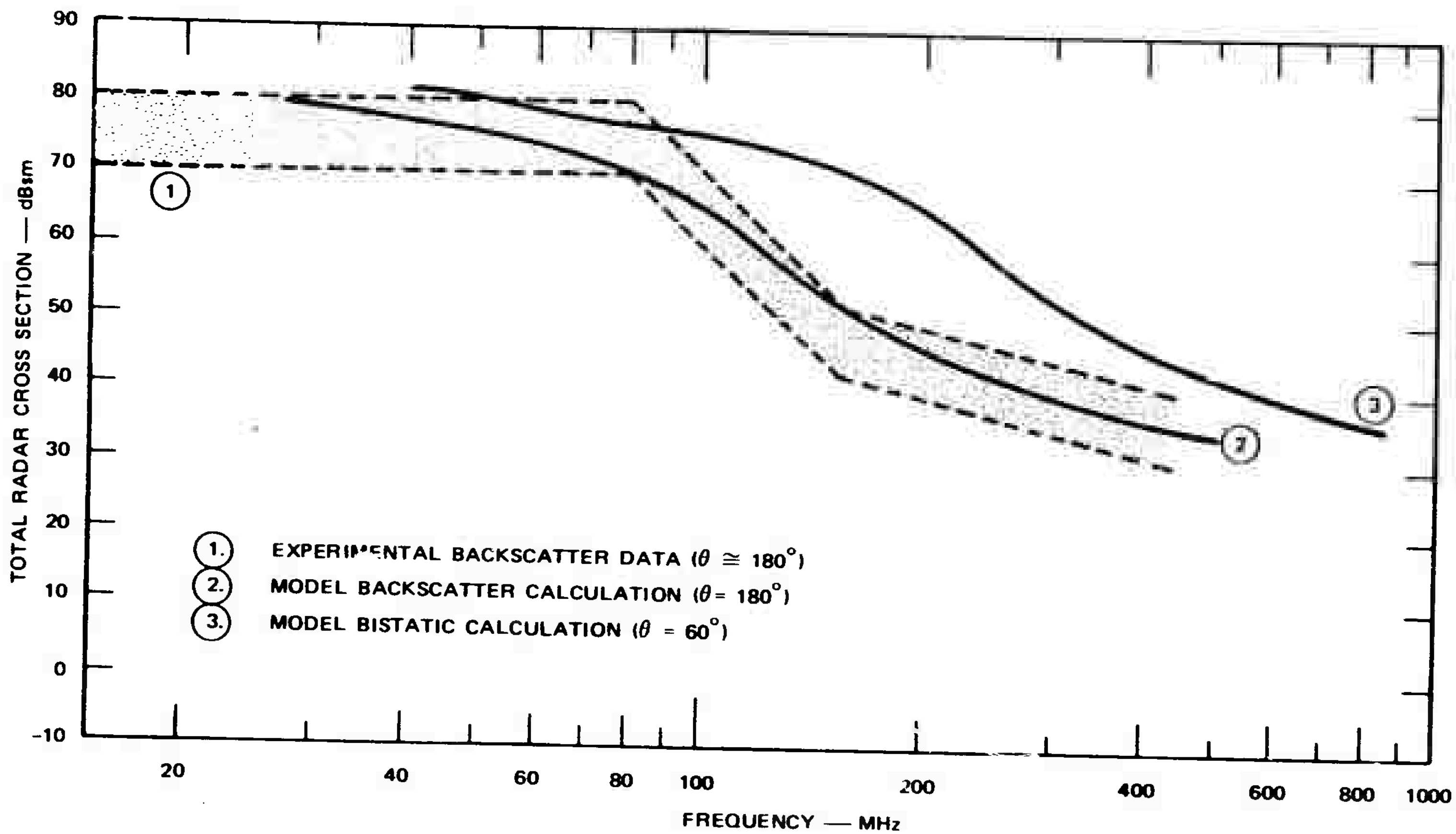

(S) FIGURE 4 MODEL BACKSCATTER AND BISTATIC CALCULATIONS COMPARED WITH EXPERIMENTAL DATA (U)

(S) Cont'd.

is that at frequencies such as 200 MHz the radar scattering cross-section over bistatic paths is expected to be as much as 20 dB greater than over backscatter paths at the same frequency.

(S) The cross-section "gain" expected over bistatic paths is a direct consequence of the Bragg scattering law and the observational fact that the backscatter cross-section decreases with increasing frequency. The Booker scattering theory views the irregularities within the heated volume as being a super position of plane sinusoidal waves in space, only one component of which is important in determining how strong the scatter will be at a particular angle and wavelength. The important component is that which satisfies specularity for the path (path bisector normal to scattering surfaces) and which has a spatial wavelength such that the scattered signal from each cycle adds constructively in the scattering direction. Constructive interference requires that the path length difference for waves scattered from adjacent planes be equal to the signal wavelength. Figure 5 shows that for bistatic paths the same irregularity component that supports near-backscatter for an operating wavelength, λ_1, will support scatter over a more bistatic path at a shorter wavelength, λ_2. The upshot of this is that the observed backscatter curve of cross-section versus frequency can be used to predict the cross-section curve over bistatic paths, using the scaling relation

$$\sigma_\theta (f) = \sigma_{180°} (f \sin \theta/2)$$

For example, if $\theta = 60°$, $\sin \theta/2 = 0.5$ and consequently the cross-section observed at frequency f over a bistatic path with $\theta = 60°$ will be the same as

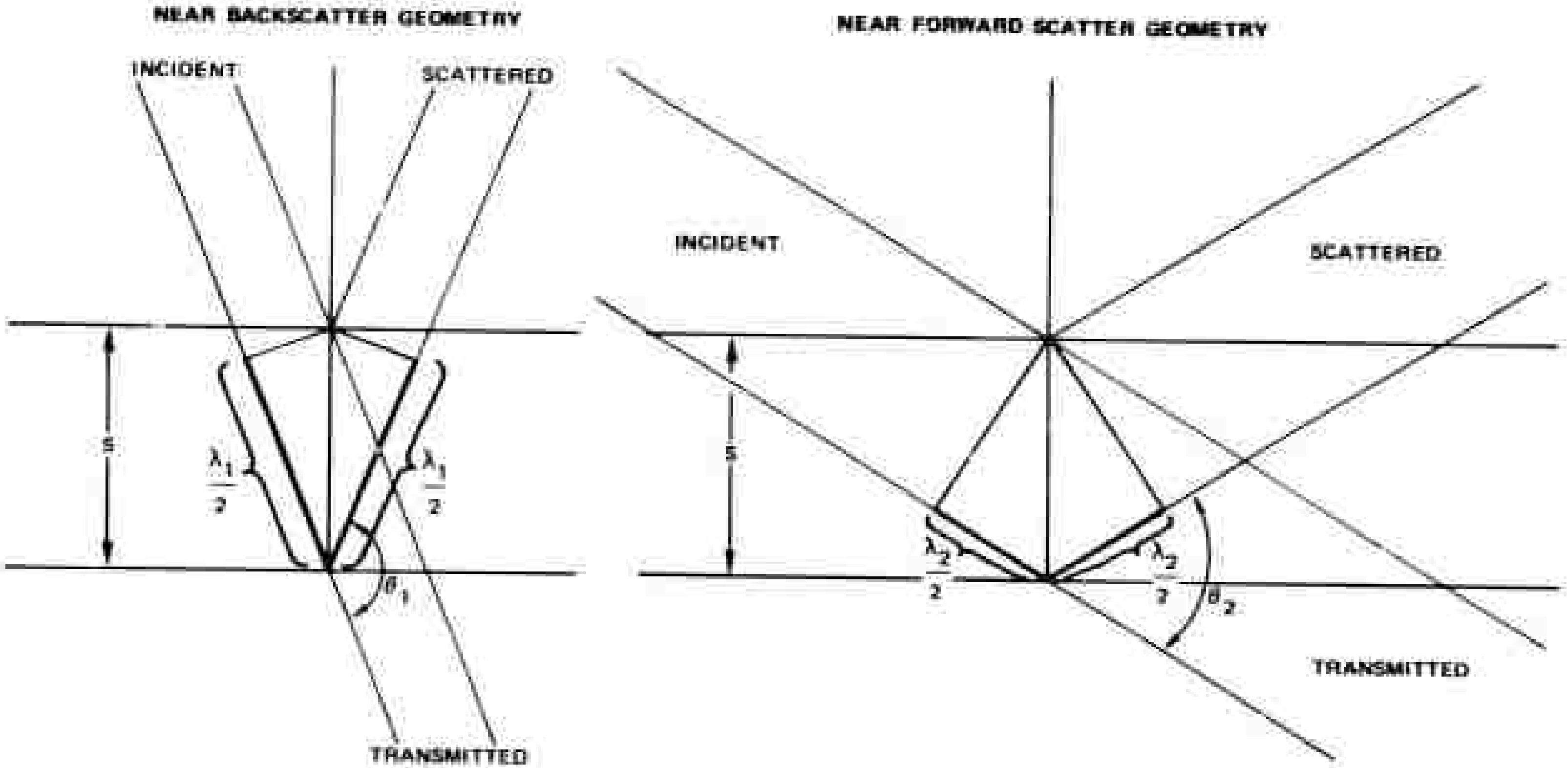

(S) FIGURE 5 BRAGG SCATTERING, SHOWING THAT THE IRREGULARITIES THAT SUPPORT BACKSCATTER AT ONE FREQUENCY SUPPORT BISTATIC SCATTER AT A HIGHER FREQUENCY (U)

(S) Cont'd.

that observed at half the frequency in backscatter. Since the cross-section increases with decreasing frequency, bistatic paths should always give a higher cross-section than backscatter paths, all else being equal. This model prediction has not been checked experimentally but plans are underway to do so.

IV SUMMARY AND CONCLUSIONS (U)

(S) An on-frequency scattering model has been developed for use over bistatic and backscatter paths. The model is consistent with the experimental data collected over backscatter or near-backscatter paths. Two important facets of the model are the following:

(S) 1. The aspect sensitivity is great enough so that for practical purposes it can be considered perfect. This means, for example, that the width of the bands along the ground where signals can be received from a remote transmitter via the heated volume are set by the finite dimensions of the scattering volume rather than by the finite correlation length of the scatterers.

(S) 2. Significantly larger radar cross-sections are predicted for bistatic geometries than for backscatter geometries at the same frequency. For example, at 200 MHz the radar cross-section of the heated volume should increase by 20 dB going from backscatter (θ = 180°) to a bistatic path (θ = 60°).

(S) The model is felt to be an important step in the right direction but is by no means complete. Except for special cases, a numerical integration must be

(S) Cont'd.

done to predict signal strengths and this will be time consuming on a computer. This drawback of the model can probably be overcome for the cases of interest by simplifying the model to the point where the integration can be done analytically. More fundamentally, the model is based upon the assumed existence of irregularities whose characteristics are chosen simply to match the observations. As the theory of the heater-ionosphere interaction is developed to the point where the characteristics of the irregularities can be predicted, the on-frequency scattering model should be revised.

REFERENCES (U)

1. Perkins, F.W., "Off-Frequency-Scattering Model", Proceeding of the Prairie Smoke, RF Scattering-Model Workshop, July 1972, SRI Technical Report, pp. 139-144, (SECRET).

2. Bowhill, S.A. and Mendenhell, E.E., "Procedures for Determining Scattering-Model Parameters", Proceeding of the Prairie Smoke RF Scattering-Model Workshop, July 1972, SRI Technical Report, pp. 95-116, (SECRET).

3. Booker, H.G., "A Theory of Scattering by Nonisotropic Irregularities with Application to Radar Reflections from the Aurora", J.A.T.P., Vol. 8, pp. 204-221, 1956, (UNCLASSIFIED).

4. Bowhill, S.A., "Geometry and Cross Sections for Bistatic Scatter", Proceedings of the Prairie Smoke RF Scattering-Model Workshop, July 1972 (U), pp. 127-137, (SECRET).

5. Pendyala, B.R., and G.D. Thome, "An RF Scattering Model for a Random Distribution of Irregularities", Proceedings of the Prairie Smoke RF Scattering-Model Workshop, July 1972 (U), pp. 57-76, (SECRET).

ON THE CHARACTERISTIC SCALE SIZES OF THE ON-FREQUENCY SCATTERING IRREGULARITIES (U)

B. R. Pendyala, G. D. Thome, and W. H. Russell

ON THE CHARACTERISTIC SCALE SIZES OF THE 'ON-FREQUENCY' SCATTERING IRREGULARITIES (U)

by

B. R. Pendyala, G. D. [illegible] and W. H. Russell

Raytheon Company
Sudbury, Massachusetts

ABSTRACT (U)

(S) The paper presents a method to extract information on the scale sizes related to longitudinal correlation and intensity of the density fluctuations from the backscatter radar observations of the angular pattern and the orientation of the reflection surface. The two parameters determine the degree to which deviations occur in the angular dimension of the radar pattern and the tilt of the reflection surface from that expected for the conditions of perfect aspect sensitivity. The curves generated of the deviations parametric in the two scale sizes show that the RAM observations are consistent with a recently reported value of 7.5 km for the intensity scale size and suggest a lower limit of about 10 m for the longitudinal correlation length defined through the relation $\theta_s = \lambda / 2\sqrt{2}\pi L$.

I INTRODUCTION (U)

(S) The 'on-frequency' scattering model presented in an earlier paper provided estimates for the transverse scale size and the intensity of the density fluctuations for the heater generated irregularities.[1] The model was based on the assumption that the signal returns are extremely aspect sensitive and hence, it turned out that the total cross section is independent of the longitudinal scale size. The intensity of the scattering irregularities is believed to be a function of height with its peak located at the height of maximum heating. Although this dependence is built into the model, no attempt has been made to obtain a scale size to describe the intensity of the density fluctuations.

(S) The information on the longitudinal correlation and the fluctuation intensity scale sizes is considered to be essential for an accurate description of the scattering model. The two parameters influence in an important manner the intensity and the angular dimension of the scattering lobe for a constant range from a diagnostic radar. The scatter returns will originate from the region where the radar looks transverse to the field aligned irregularities and the scattering lobe will have the dimension of the antenna pattern for the conditions of perfect aspect sensitivity. Any deviation from this exact situation is a direct consequence of the finite aspect sensitivity which in turn results from the finiteness of the longitudinal correlation scale size. When the irregularities are highly aspect sensitive, the primary effect of the height dependence of the density fluctuations is to cause the intensity of the scattered signal to change as a function of mismatch between the heater and the specular reflection heights. An estimate has been made of the scale size for the

(S) Cont'd.

fluctuation intensity by Sweeney and Fialer using the observations of the signal intensity variation with the height mismatch.[2] A somewhat less obvious effect is to introduce a slight shift in the angular position of the maximum return in the direction of the heater reflection height from the point of exact specularity. Thus the effects of the two parameters, which in fact are coupled, will reflect in the deviations in the orientation of the reflection surface and the angular width of the scattered return from that corresponds to the condition of perfect aspect sensitivity. This paper is devoted to the simulation of the scattering patterns for RAM radar and to extract some information on the two parameters.

II SIMULATION OF RADAR PATTERNS (U)

(S) The observed angular pattern of the signal intensity is the result of the convolution of the radar beam with the scattering pattern of the irregularities. Hence the intensity pattern $I(\theta_o)$ for an antenna scan parallel to the magnetic field (elevation scan for RAM) is expressed as:

$$I(\theta_o) = K \int_{-\pi}^{+\pi} G_a^2 (\theta-\theta_o) G_s (\theta) d\theta \qquad (1)$$

where, as illustrated in Figure 1,

$G_a(\theta)$ = antenna pattern of the radar

$G_s(\theta)$ = scattering pattern of the irregularities

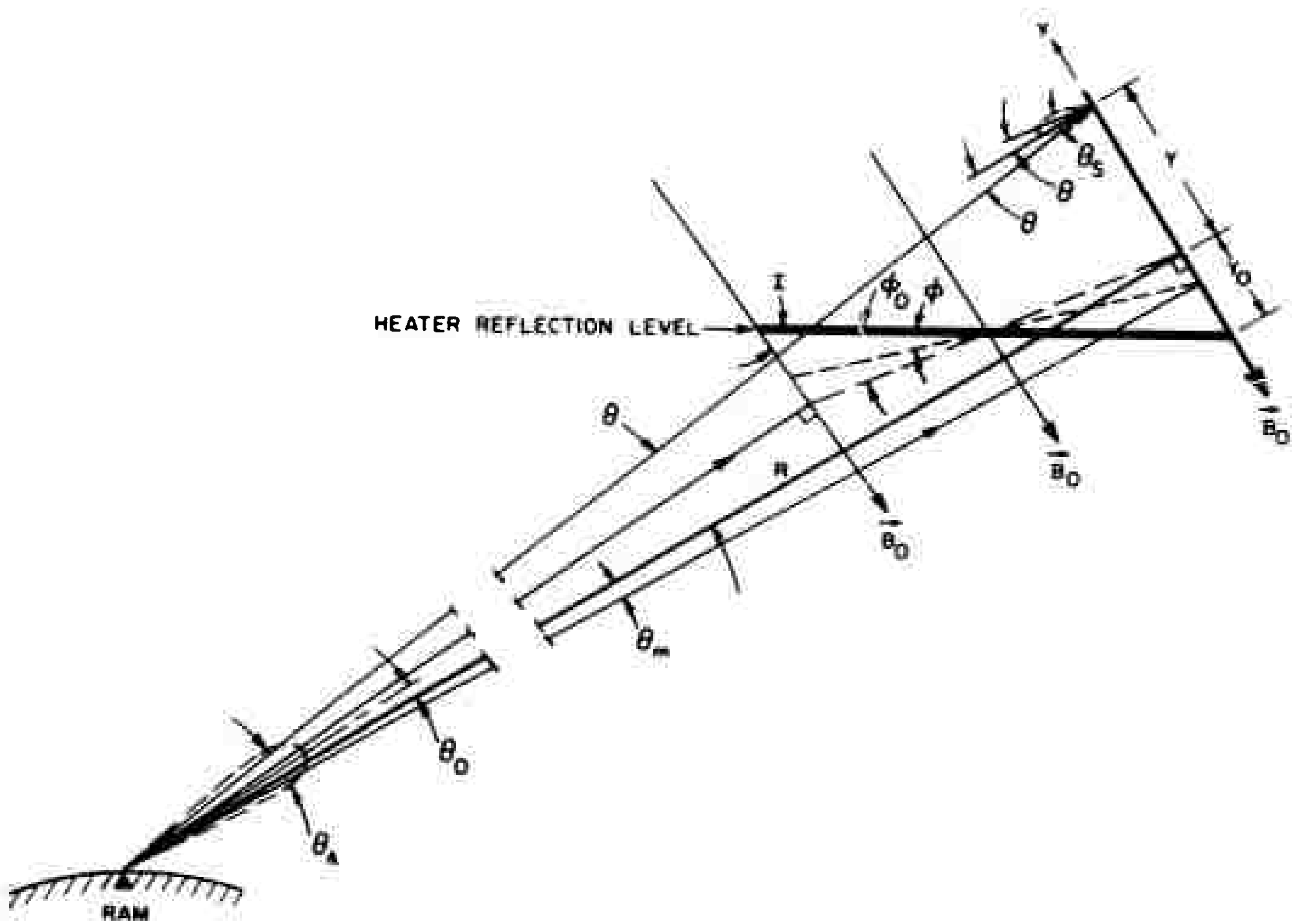

(S) FIGURE 1. ILLUSTRATION TO SHOW THE GEOMETRY USED IN COMPUTING THE RECEIVED POWER PATTERN AND THE SLOPE OF THE SCATTERING DISK (S)

(S) Cont'd.

θ_o = elevation angle of the radar beam from the direction of specularity

θ = elevation angle to a scattering irregularity

and K = a constant relate t. system parameters

Let the radar beam and the scattering patterns be of Gaussian shape such that:

$$G_a = G_{ao} \exp \left\{ -(\theta-\theta_o)^2/\theta_a^2 \right\} \quad (2)$$

and

$$G_s = G_s(y) \exp \left\{ -(2\theta/\theta_s)^2 \right\} \quad (3)$$

Where θ_a and θ_s are the e-folding beamwidths of the antenna and the scattering patterns. $G_s(y)$ is the scattering lobe intensity corresponding to the intensity variation of the irregularities as function distance along the magnetic field. Let us assume

$$G_s(y) = G_{so} \exp \left\{ -(y-y_0)^2/A^2 \right\} \quad (4)$$

where, as shown in Figure 1,

y_0 = distance of the heater reflection from the specular point

y = distance from the specular point to the scattering irregularity

and A = Gaussian scale size for the intensity variation of the irregularities along the magnetic field

(S) Cont'd.

The high aspect sensitivity of the irregularities, limiting the scattering to a spatial extent small compared to the radar range, permits the approximation $\theta \approx y/R$ for evaluating the integral in Equation (1). On substituting the above relations and evaluating the integral one obtains the following for the signal intensity pattern:

$$I(\theta_o) = \frac{K\sqrt{\pi}}{S} \exp\left\{-(y_o/A)^2 - (2\theta_o^2/\theta_a^2) + \left[\frac{2R\theta_o}{S(R\theta_a)^2} + \frac{y_o}{SA^2}\right]^2\right\} \quad (5)$$

where

$$S = \left[\frac{2}{(R\theta_a)^2} + \frac{4}{(R\theta_s)^2} + \frac{1}{A^2}\right]^{1/2}$$

The angular position θ_m of the peak of the intensity pattern is obtained by solving for θ_o satisfying the equation $dI(\theta_o)/d\theta_o = 0$. The solution for θ_m is given as:

$$\theta_m = 2Ry_o\theta_a^2/A^2\left[2S^2(R\theta_a)^2 - 4\right] \quad (6)$$

The intensity distribution is expressed in the normalized form as:

$$I_n(\theta_o) = I(\theta_o)/I(\theta_m) \quad (7)$$

using Equations (5) and (7) the normalized intensity patterns can be computed parametric in A and L, the scale sizes for the fluctuation intensity and the longitudinal correlation of the irregularities. The correlation length L is related to the scattering lobe size θ_s as[3]:

$$\theta_s = \lambda/2\sqrt{2}\pi L \quad (8)$$

(S) Cont'd.

Where λ is the wavelength of the operating radar. Figure 2 presents a set of curves parametric in L showing the variation of θ_s with the operating frequency. The angular dimension and the slope of the scattering disk of irregularities are determined from the computed normalized intensity patterns $I_n(\theta_o)$. The tilt of the scattering disk is determined from the angular position θ_m of the peak of the intensity pattern.

III NUMERICAL RESULTS (U)

(S) The following parameters relevant to the RAM radar observations are used to compute the intensity patterns:

$$R = 900 \text{ km}$$

$$\theta_a = 3.46°$$

$$f = 157.5 \text{ MHz}$$

$$y_o = -10 \text{ km}$$

The patterns are calculated parametric in the scale sizes A and L. The computed values of the angular width and the tilt angle of the scattering disk are normalized by the antenna beamwidth and the tilt of the specular scattering surface and the results are presented in Figure 3. The curves generated correspond to the scale sizes A ranging from 5 to 100 km and L from 2.5 to 16 m. The dependence of the width and the tilt of the scattering disk on the scale size parameters is found to be sensitive enough to extract information on the scale sizes from the backscatter radar measurements. It is recognized, however, that at very high operating frequencies the observed deviations from the conditions of perfect aspect sensitivity are very small and the method relies on a

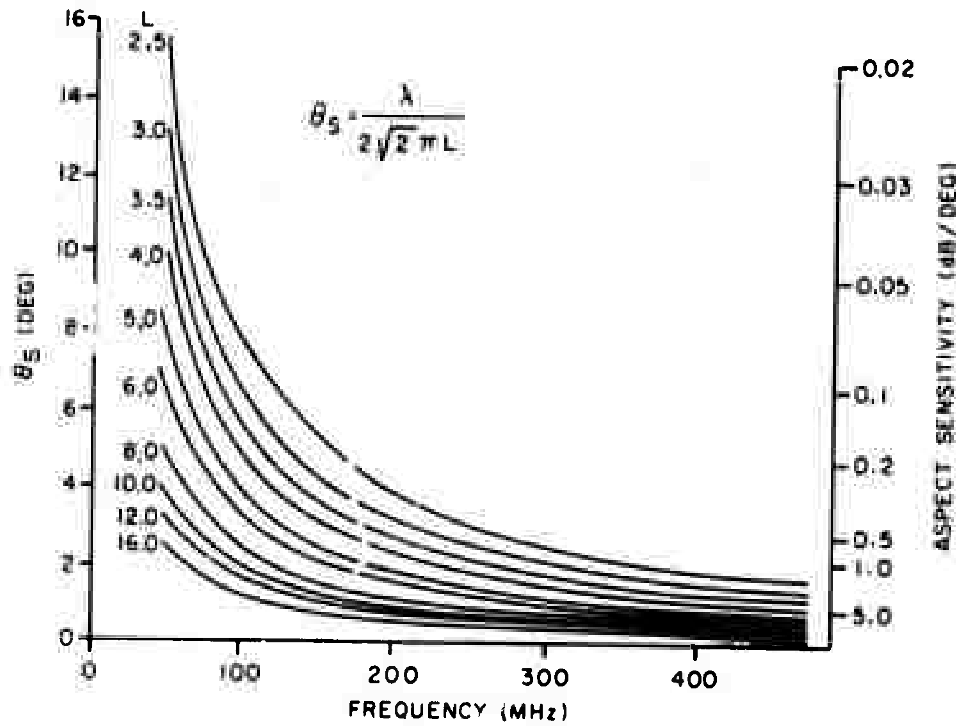

(U) FIGURE 2. FREQUENCY DEPENDENCY OF THE ASPECT SENSITIVITY OF THE SCATTERING IRREGULARITIES PARAMETRIC TO THE LONGITUDINAL AUTOCORRELATION LENGTH L (U)

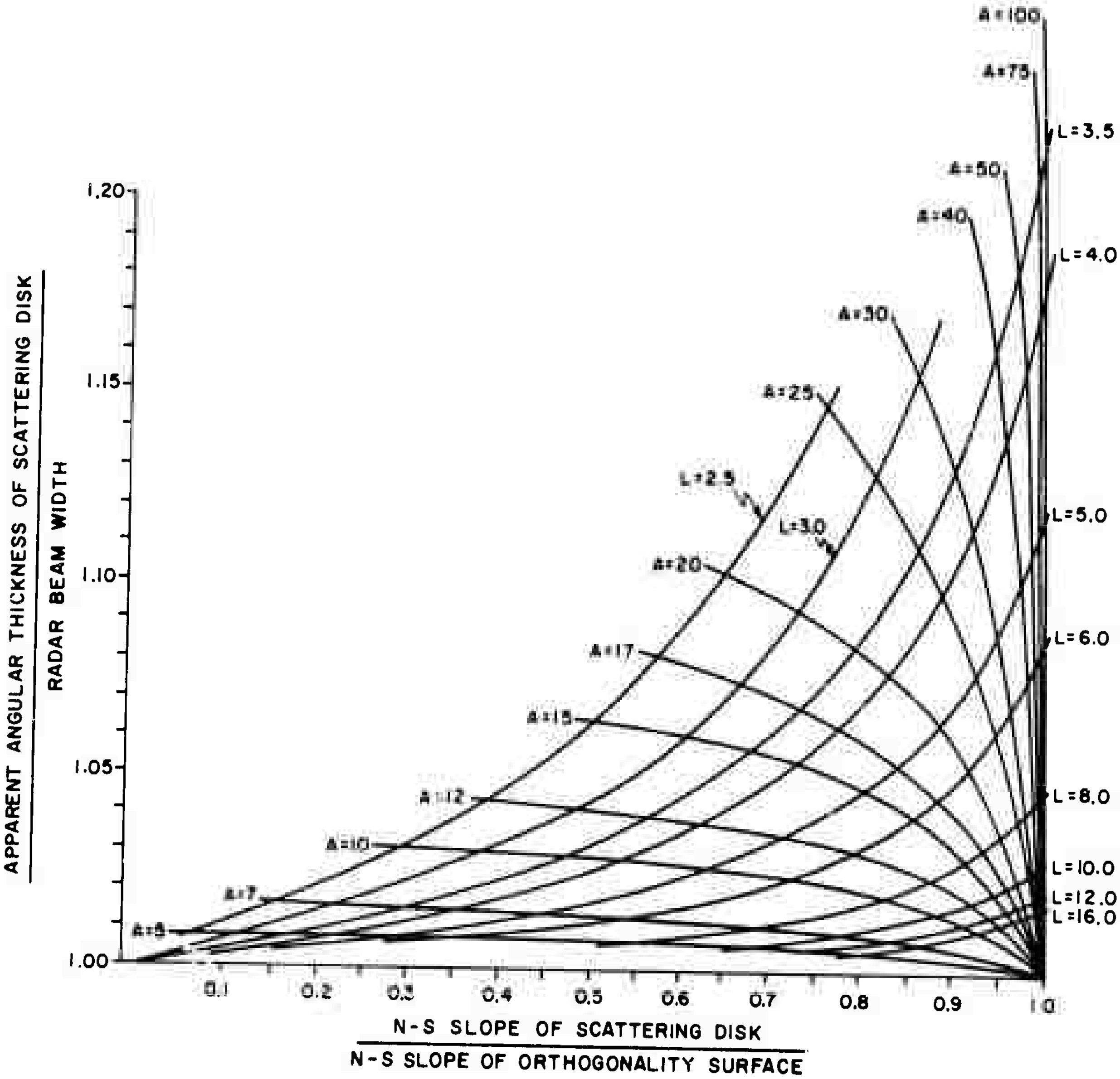

(S) FIGURE 3. THE NORMALIZED ANGULAR DIMENSION A AND THE SLOPE OF THE SCATTERING DISK PARAMETRIC IN THE SCALE SIZES A AND L (S)

(S) Cont'd.

high degree of precision in the measurements. The received power pattern in elevation scan observed by Minkoff et. al[4] using the RAM radar during a Prairie Smoke II test conducted on April 25, 1972 is shown in Figure 4. The circles represent the received power and the crosses denote the square of the antenna pattern corresponding to a point source response for the backscatter operation. The dotted curves represent 10% and 20% broadening over the antenna pattern. The observations do suggest that the broadening due to finite aspect sensitivity of the scatterers is almost negligible and may be not more than 5% at the most. The results on the tilt angle of the scattering disk are taken from the observations collected at RAM on 12, 13 and 14 of October 1971.[5] The observed tilt angles normalized to the tilt angle of the specular surface are shown in Figure 5 for nine different cases. It may be seen from the figure that the deviation of the observed tilt angle relative to the specular surface is 15% or less. The observations are found to be consistent with a recently reported estimate of 7.5 km for A in that it requires only a little over 1% broadening in the measured pattern. Commensurate with these parameters and a 15% deviation in the tilt angle, the curves suggest a lower limit of about 10 m for the correlation scale size L.

IV CONCLUSION (U)

(S) It is shown that the backscatter radar observations of the angular dimension of the radar pattern and the tilt of the reflection surface can be used to extract information on the characteristic scale sizes describing the longitudinal correlation and the intensity variation of the density fluctuations.

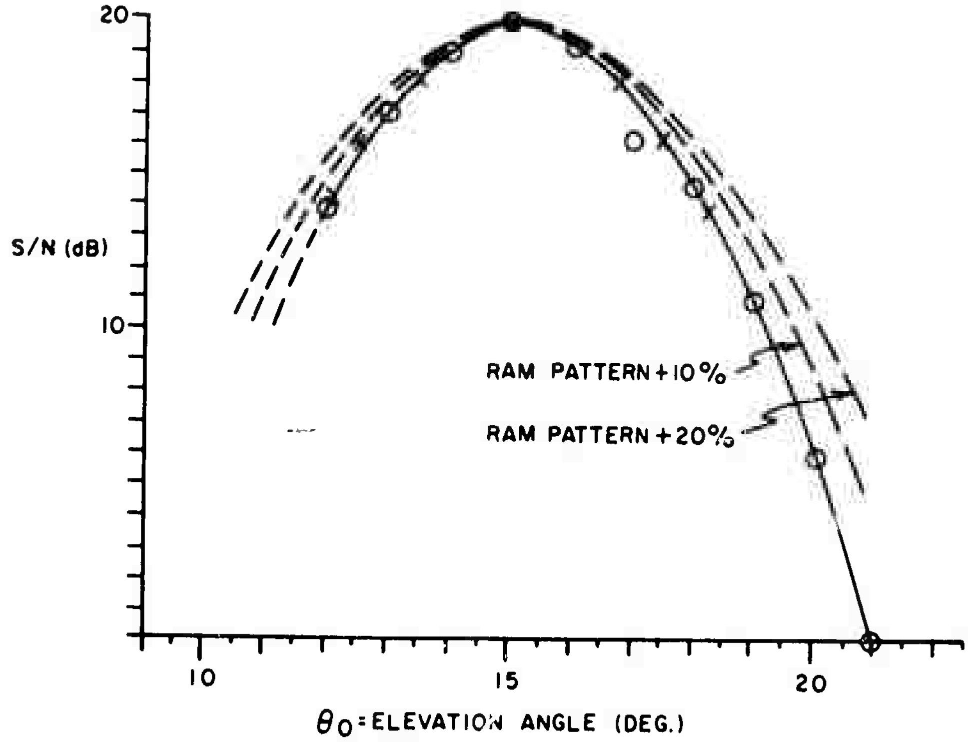

FIGURE 4. RECEIVED POWER VERSUS ELEVATION ANGLE OBSERVED AT RAM ON 25 APRIL 1972 ALONG WITH CURVES SHOWING 10% and 20% PATTERN BROADENING (S)

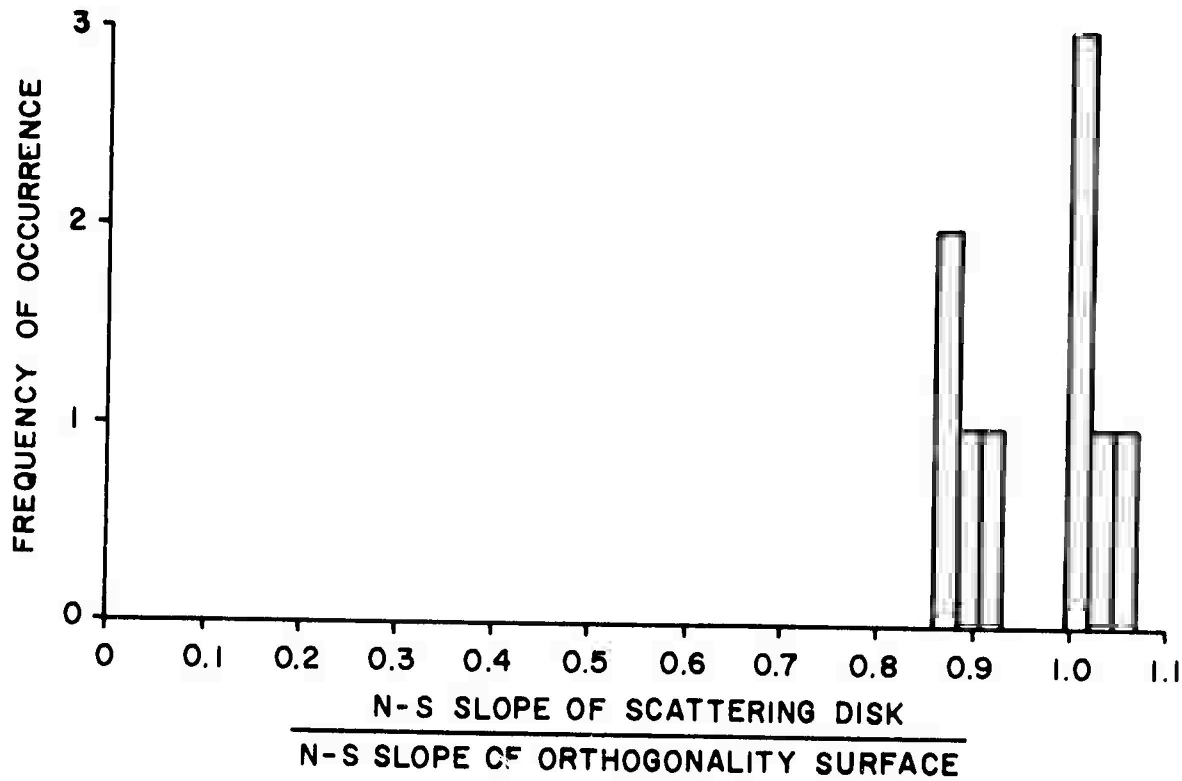

(S) FIGURE 5. DISTRIBUTION OF THE NORMALIZED SLOPE OF THE SCATTERING DISK OBSERVED AT RAM ON 12, 13 AND 14 OCTOBER 1971 (S)

(S) Cont'd.

RAM observations are found to be consistent with a value of 7.5 km for the intensity scale size and seem to suggest a lower limit of 10 m for the longitudinal correlation length as defined by Booker.[3]

REFERENCES (U)

1. Pendyala, B.R. and G.D. Thome, An RF Scattering Model for a Random Distribution of Irregularities, Proc. of the Prairie Smoke, RF - Scattering - Model Workshop, SRI Technical Report, September 1972 (SECRET).

2. Sweeney, Jr., L.E. and P.A. Fialer, The Empirical Model, Proc. of the Prairie Smoke, RF - Scattering - Model Workshop, SRI Technical Report, September 1972 (SECRET).

3. Booker, H.G., "A Theory of Scattering by Nonisotropic Irregularities with Application to Radar Reflections from the Aurora", JATP, 8, 204, 1956 (UNCLASSIFIED).

4. Minkoff, J.B., Kugelman, P. and Laviola, M., "Preliminary Summary of Results of Prairie Smoke II Experiments (U)", RRI Research Memorandum M-2/174-4-50, 1 June 1972 (SECRET).

5. Minkoff, J.B. and Kugelman, P., "Preliminary Summary of Results of Ivory Coral Experiments (U)", RRI Technical Memorandum TM-38/174-4-50, 29 December 1971 (SECRET).

DIMENSIONS OF GROUND ILLUMINATION PATTERNS (U)

W. H. Russell, B. R. Pendyala, and G. D. Thome

DIMENSIONS OF GROUND ILLUMINATION PATTERNS (U)

by

W. H. Russell, B. R. Pendyala and G. D. Thome

Raytheon Company
Sudbury, Massachusetts

ABSTRACT

(S) This paper presents a method for computing the ground illumination patterns for 'on-frequency' scatter from the heated volume. The size of the illumination zones in a north-south plane are calculated by considering their dependency on the operating frequency, the size of the scattering volume and the aspect sensitivity of the scatterers. The results show that the size of the illumination zones are primarily dependent on the finite size of the scattering volume rather than on the finite aspect sensitivity of the scatterers.

I INTRODUCTION (U)

(S) Aircraft observations of scatter from the heated region during June of 1971 have shown that adequate reception of the scattered energy is possible only within specific zones on the ground.[1] These regions are typically 200 to 250 km wide in the north-south direction but considerably larger in the east-west direction. It was postulated at that time that the size of the north-south zone was dependent primarily on the size of the scattering volume.[2] Experimental evidence also showed that operating frequency influenced the zone size and that refraction apparently affects the location of the zones. Other factors such as the aspect sensitivity and the propagation geometry will also influence the size of the illumination area and its location.

II COMPUTATION OF GROUND ILLUMINATION PATTERNS (U)

(S) To investigate some of these interdependencies, the scattering process has been modeled analytically so that the relative intensity of the scatter on the ground could be evaluated. To examine only the size of the zone and how it varies with operating frequency and the size of the heated volume, some approximations have been made. The frequency dependency has been restricted to the VHF spectrum so that refraction effects can be neglected. Also the scattering geometry has been constrained to a plane containing the heated region and the radar. These approximations permit a two dimensional straight line description of the scattering process. Furthermore, the magnetic field has been considered constant throughout the heated volume and the curvature of the earth was neglected.

(S) Within the above constraints, the resulting geometry of the scattering may be described by Figure 1. The intensity of heater produced irregularities is considered maximum at point O and decreases in a Gaussian fashion in the x and z direction with scale sizes of W and A respectively.

(S) The intensity, ΔI, at a point Q on the ground due to a scatterer at P is, therefore, dependent on the location of P in the scattering volume so that ΔI may be set proportional to the following term, (see Figure 1)

$$e^{-(x^2/W^2)}\; e^{-(z + x \cos I)^2/A^2} \tag{1}$$

The intensity will also be influenced by the scattering pattern of the irregularities at P. For a Gaussian scattering pattern of the irregularities with a 1/e beamwidth of θ_s, the effect of aspect sensitivity on the relative intensity at Q may be described by an expression of the form

$$e^{-(S/R\theta_s)^2} \tag{2}$$

where S and R may be formulated in terms of the geometry as: (see Figure 1)

$$S = 2z - \frac{zd \sin I}{R_o + x \sin I} + d \cos I \tag{3}$$

and

$$R = R_o + (x - d) \sin I \tag{4}$$

The relations in Equations 3 and 4 are appropriate for the case of high aspect sensitivity and when it is assumed that R_o is long compared to the scattering volume size and the ground distance d.

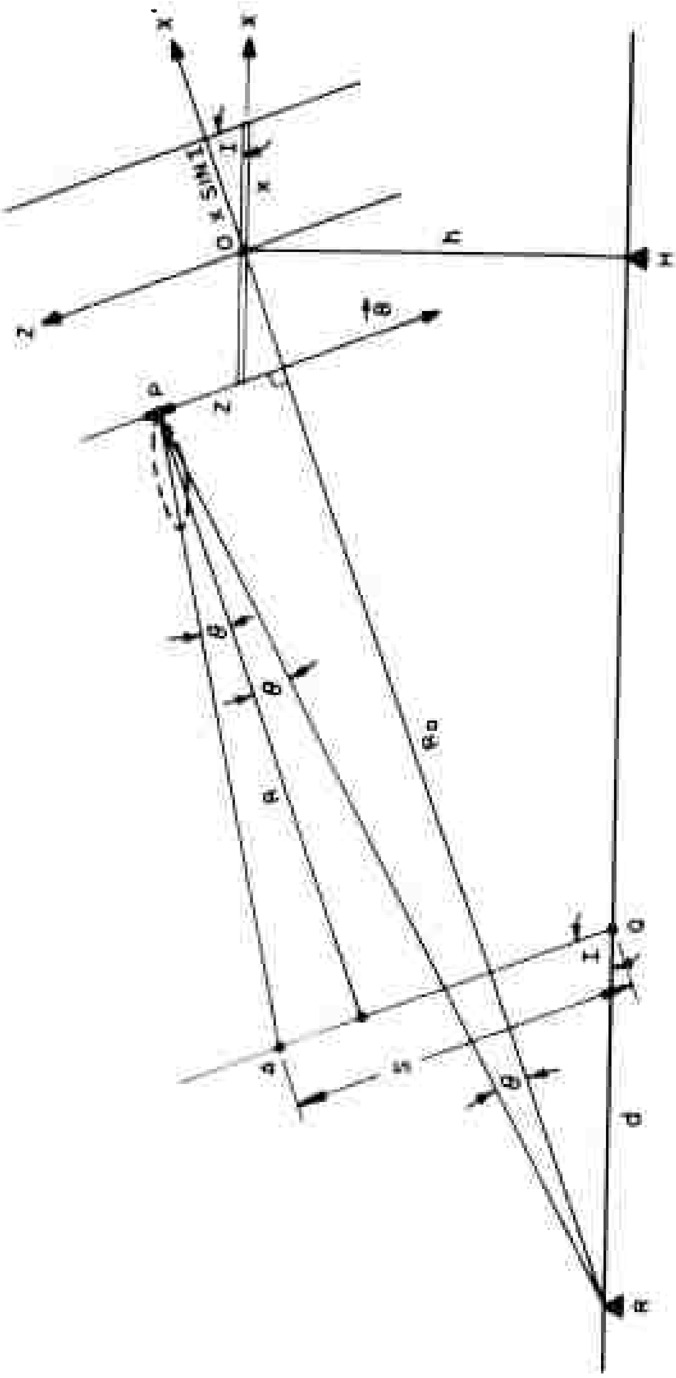

(S) FIGURE 1. AN ILLUSTRATION TO SHOW THE GEOMETRY USED IN COMPUTING THE GROUND ILLUMINATION PATTERNS (S)

(S) From the expressions 1 and 2 the intensity at Q due to the scatterer at P is given as:

$$\Delta I = I_m\, e^{-x^2/W^2}\, e^{-(z + x \cos I)^2/A^2}\, e^{-(S/R\theta_s)^2} \qquad (5)$$

Evaluating the above expression for various values of d provides a distribution of the intensity on the ground due to scatter from a single irregularity at P. The resulting distribution will not only be dependent on the geometry but also on the operating frequency through the aspect sensitivity term θ_s, since[3]:

$$\theta_s = \lambda/2\sqrt{2}\pi L \qquad (6)$$

where

λ = operating wavelength

L = autocorrelation length as defined by Booker

A distribution in d may also be obtained for the scatter due to a column of irregularities along the field lines by integrating Equation 5 over all z so that

$$I = \frac{\pi I_m\, e^{N^2}}{N}\, e^{-x^2/W^2}\, e^{-x^2\cos^2 I/A^2}\, e^{-d^2\cos^2 I/\theta_s R^2} \qquad (7)$$

where

$$M = \left\{\frac{1}{A^2} + \left[2 - \frac{d \sin I}{R_o + X \sin I}\right]^2 /\theta_s^2 R^2\right\}^{1/2}$$

and

$$N = \left\{\frac{x \cos I}{A^2} + \left[\left(2 - \frac{d \sin I}{R_o + x \sin I}\right) d \cos I\right] /\theta_s^2 R^2\right\} /M$$

(S) In a similar manner, a distribution of the intensity on the ground due to scatter from a heated area may be obtained by integrating the effect of scatterer along z and also x. The integration in the x dimension, however, has been accomplished by a numerical technique.

(S) To illustrate this approach, the intensity distributions have been computed for a geometry appropriate to that of the RAM backscatter observations of the irregularities over the Platteville heater. Computations of the distributions were made at 50, 100 and 150 MHz for a single irregularity at the center of the heated region, a column of irregularities through the center of the heated volume, and for a total area of scatterers centered over the heater. The parameters chosen to compute these distributions are as follows:

$A = 7.5$ km $R = 900$ km

$W = 50$ km $I = 68°$

The results are shown in Figure 2, where the areas under the distribution curves are shaded to distinguish between the three conditions considered above (solid = single irregularity, dark dots = column, and light dots = total area). It is apparent from Figure 2 that consideration of a large scattering area produces a substantial distribution on the ground. The distributions generated from the integration over the total heated area are approximately 235 km wide between 6 dB points which compares favorably with the experimental observations of zone sizes of approximately 200 to 250 km. It may also be noted from Figure 2 that these distributions are all approximately of the same size regardless of frequency. This condition exists since any broadening of the distributions due to finite highly aspect sensitive scattering patterns of the individual

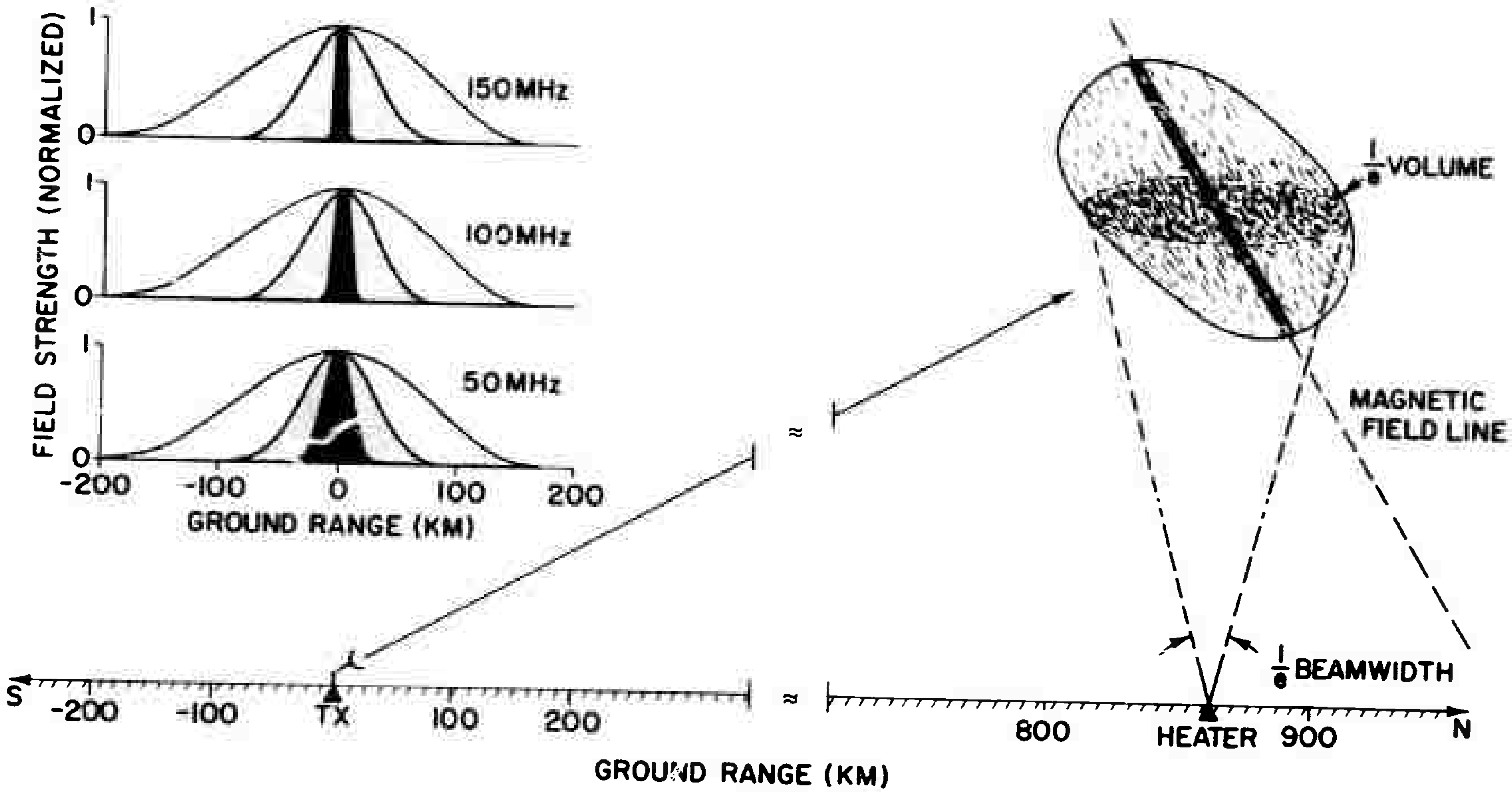

(S) FIGURE 2. THE EFFECT OF THE DIMENSION OF THE SCATTERING VOLUME AND THE OPERATING FREQUENCY ON THE GROUND ILLUMINATION PATTERNS (S)

(S) Cont'd.

irregularities is small compared with the effect of the total scattering volume.

III CONCLUSIONS (U)

(S) The results presented here suggest that the size of the ground illumination pattern for on-frequency scattering from the heated volume is controlled primarily by the finite size of the scattering volume rather than by the finite aspect sensitivity of the individual scatterers.

REFERENCES (U)

1. Minkoff, J. and Kugelman, P., "Preliminary Summary of Results of Ivory Coral Experiments (U)", Riverside Research Institute, Technical Memorandum TM-38/174-4-50, December 1971 (SECRET).

2. Blood, D.W., "White Sands Ivory Coral Observations During June 1971 (U)", Ivory Coral Report No. 3, ER72-4017, RADC-TR-72-43, Contract F30602-68-C-0299, January 1972 (SECRET).

3. Booker, H.G., "A Theory of Scattering by Nonisotropic with Application to Radar Reflections from the Aurora", JATP, Vol. 8, 1956. (UNCLASSIFIED).

RF SCATTERING MODEL SUMMARY AND CONCLUSIONS (U)

G. D. Thome, B. R. Pendyala, and W. H. Russell

RF SCATTERING MODEL SUMMARY AND CONCLUSIONS (U)

by

G. D. Thome, B. R. Pendyala and W. H. Russell

Raytheon Company

Sudbury, Massachusetts

(S) An RF scattering model which is consistent with the existing experimental measurements has been developed for the 'on-frequency' signal component scattered from the heater induced ionospheric irregularities. The model is intended primarily for scatter communication systems application and further to aid in the theoretical and experimental efforts to understand the heater-ionosphere interaction phenomenon.

(S) The model presented here is based on the theory of weak scattering (Born approximation) developed by Booker for the case of anisotropic field aligned Gaussian irregularities. The same type of functional form has been adopted in the model to characterize the heater induced 'on-frequency'scattering irregularities. No attempt has been made to justify how such type of irregularities are produced or maintained and to this extent it might become necessary to modify the model in future when a complete theoretical description of the irregularities is made available.

(S) The characteristics of the irregularities in the heated volume are specified generally by a two dimensional Gaussian autocorrelation function having

(S) Cont'd.

a scale size T transverse to the magnetic field and a scale size L along the field. These two parameters along with the intensity of the density fluctuations determine the scattering properties of the disturbance. Essentially, it is the transverse scale size that governs the frequency dependence whereas the ratio (L/T) determines the aspect sensitivity of the scatterers. In order to be able to match the model computations with the observations of total scattering cross section as function of radar frequency, it was found essential to assume that two dominant sets of irregularities with transverse scale sizes T_1 and T_2 are present in the scattering volume. Using a highly refined earth's magnetic field model and the observations of the distribution of signal returns in space, it was shown that the on-frequency scatterers are extremely aspect sensitive. This property has been used to effect substantial simplification in analytical evaluation of the scattering coefficient integral. The total backscatter radar cross section for two scale size scattering medium was derived as:

$$\sigma_T = \frac{4\pi^5 W^2 R\lambda\,(\Delta N/N)_o^2}{\lambda_N^4} \exp\left\{-D^2/A^2\right\} \left(\alpha\, T_1^2 \exp\left[\frac{-8\pi^2 T_1^2}{\lambda^2}\right] + (1-\alpha)\, T_2^2 \exp\left[\frac{-8\pi^2 T_2^2}{\lambda^2}\right] \right)$$

where

R = range from radar to the specular point in the scattering volume

λ = radar wavelength

(S) Cont'd.

λ_N = ambient plasma wavelength at the specular point

W = Gaussian radius of the heated volume in a horizontal plane at the reflection level

$\overline{(\Delta N/N)_o^2}$ = mean square electron density fluctuations of the irregularities at the specular point

A = Gaussian scale size of $\overline{(\Delta N/N)^2}$ along the magnetic field

D = separation along the field between the specular point and the heater reflection level

T_1, T_2 = Gaussian autocorrelation scale sizes for density fluctuations transverse to the magnetic field

α = a parameter determining the relative strength of the two Gaussian irregularity distributions used in the model

(S) The model predictions were found to match well with the observed optimum radar cross sections when the values assigned to various parameters are as follows:

R	= 900 km	$\overline{(\Delta N/N)_o^2}$	= 0.6×10^{-4}
λ_N	= 54 m	T_1	= 0.1 m
W	= 90 km	T_2	= 0.5 m
D	= 0	α	= 0.24

(S) The model discussion as indicated above was limited essentially to the backscatter case although an approach to obtain a general solution for a bistatic situation was also presented. While the exact solution is quite involved it can be shown using the principle of Bragg scattering that to the first order of approximation the radar cross section for a bistatic path can

(S) Cont'd.

be expressed in terms of an equivalent backscatter cross section using the scaling relation

$$\sigma_\theta\ (f;\ R_1,\ R_2) = \sigma_{180}\ (f \sin \theta/2,\ R)$$

Where θ is the scattering angle and R is the equivalent backscatter range related to the bistatic ranges R_1 and R_2 as:

$$R = 2\ R_1\ R_2 \sin (\theta/2)/(R_1 + R_2)$$

The scaling relation predicts that the bistatic radar cross sections are significantly greater than that for backscatter at the same frequency as a consequence of the fact that the radar cross section increases with decreasing frequency. For example, at 200 MHz the radar cross section of the heated volume should increase by approximately 20 db going from backscatter (θ = 180°) to a bistatic path (θ = 60°). This model prediction is now in the process of being checked experimentally.

(S) The model as described above has not provided any information on two of the scale size parameters, L and A, describing the longitudinal correlation and the intensity variation of the density fluctuations. A method was presented to extract the scale sizes from the backscatter radar observations of the angular pattern and the orientation of the scattering surface. The two parameters determine the degree to which deviations occur in the observed radar patterns from that expected for the conditions of perfect aspect sensitivity. The curves generated of the deviations parametric in the two scale sizes show that the RAM radar observations are consistent with a recently reported value

(S) Cont'd.

of 7.5 km for the intensity scale size and suggest a lower limit 10 m for the longitudinal correlation length defined through the relation $\theta_s = \lambda / 2\sqrt{2}\pi L$.

(S) The final aspect of the scattering model presented in this report is related to the dimensions of the ground illumination patterns due to the 'on-frequency' scatter from the heated volume. The sizes of the illumination zones in a north-south plane are calculated by considering their dependency on the operating frequency, the size of the scattering volume and the aspect sensitivity of the scatterers. The results show that the size of the illumination zones are primarily dependent on the finite size of the scattering volume rather than on the finite aspect sensitivity of the scatterers.

SECRET
Security Classification

DOCUMENT CONTROL DATA - R & D

(Security classification of title, body of abstract and indexing annotation must be entered when the overall report is classified)

1 ORIGINATING ACTIVITY (Corporate author) Raytheon Company Equipment Development Laboratory Sudbury, MA 01776	2a. REPORT SECURITY CLASSIFICATION SECRET 2b. GROUP XGDS - 3

3 REPORT TITLE

Scattering Model Development (U)

4 DESCRIPTIVE NOTES (Type of report and inclusive dates)

Final Report

5 AUTHOR(S) (First name, middle initial, last name)

George D. Thome
B. Rao Pendyala
William H. Russell

6 REPORT DATE	7a. TOTAL NO. OF PAGES	7b. NO. OF REFS
December 1972	75	25

8a. CONTRACT OR GRANT NO. F30602-72-C-0261	9a. ORIGINATOR'S REPORT NUMBER(S) ER72-4496
b. PROJECT NO. ARPA Order #1423	
c.	9b. OTHER REPORT NO(S) (Any other numbers that may be assigned this report)
d.	RADC-TR-73-15

10 DISTRIBUTION STATEMENT

11 SUPPLEMENTARY NOTES Monitored by Richard A. Schneible (315)330-3451 RADC (OCSE) GAFB NY 13441	12. SPONSORING MILITARY ACTIVITY Defense Advanced Research Projects Agency Arlington, VA 22217

13. ABSTRACT

(S) An RF scattering model which is consistent with existing IVORY CORAL and PRAIRIE SMOKE experimental measurements has been developed for the 'on frequency' signal component scattered from the heater induced ionospheric irregularities. The model is intended primarily for scatter communications systems application and further to aid in the theoretical and experimental efforts to understand the heater-ionsphere interaction phenomenon.

(S) The model presented here is based on the theory of weak scattering (Born approximation) developed by Booker for the case of anisotropic field aligned Goussian irregularities. The characteristics of the irregularities in the heated volume are specified generally by a two dimensional Gaussian autocorrelation function having a scale size T transverse to the magnetic field and a scale size L along the field. The model predictions were found to match well with the observed radar cross-sections.

DD FORM 1 NOV 66 1473

SECRET
Security Classification

14 KEY WORDS	LINK A		LINK B		LINK C	
	ROLE	WT	ROLE	WT	ROLE	WT
Ionospheric modification						
Ionospheric heating						
Ionospheric scatter propagation						
Booker model						
Field-aligned scattering						